

Modulational electrostatic wave-wave interactions in plasma fluids modeled by asymmetric coupled nonlinear Schrödinger (CNLS) equations

N. Lazarides¹, Giorgos P. Veldes², Amaria Javed³, Ioannis Kourakis^{1,4,5}

¹ Department of Mathematics, Khalifa University of Science and Technology,
P.O. Box 127788, Abu Dhabi, UAE

² Department of Physics, University of Thessaly, Lamia 35100, Greece

³ Center for Quantum and Topological Systems,

New York University Abu Dhabi, P.O. Box 129188, Abu Dhabi, UAE

⁴ Space and Planetary Science Center, Khalifa University of Science and Technology,
P.O. Box 127788, Abu Dhabi, UAE

⁵ National and Kapodistrian University of Athens, Faculty of Physics,
School of Science, Panepistimiopolis, Zografos 157 84 Athens, Greece

(Dated: March 26, 2024)

The interaction between two co-propagating electrostatic wavepackets characterized by arbitrary carrier wavenumber is considered. A one-dimensional (1D) non-magnetized plasma model is adopted, consisting of a cold inertial ion fluid evolving against a thermalized (Maxwell-Boltzmann distributed) electron background. A multiple-scale perturbation method is employed to reduce the original model equations to a pair of coupled nonlinear Schrödinger (CNLS) equations governing the dynamics of the wavepacket amplitudes (envelopes). The CNLS equations are in general asymmetric for arbitrary carrier wavenumbers. Similar CNLS systems have been derived in the past in various physical contexts, and were found to support soliton, breather, and rogue wave solutions, among others. A detailed stability analysis reveals that modulational instability (MI) is possible in a wide range of values in the parameter space. The instability window and the corresponding growth rate are determined, considering different case studies, and their dependence on the carrier and the perturbation wavenumber is investigated from first principles. Wave-wave coupling is shown to favor MI occurrence by extending its range of occurrence and by enhancing its growth rate. Our findings generalize previously known results usually associated with symmetric NLS equations in nonlinear optics, though taking into account the difference between the different envelope wavenumbers and thus group velocities.

I. INTRODUCTION

The theoretical and experimental investigation of plasma dynamics has grown significantly in the last decades, because of their vast application prospects related to Space and fusion plasmas, among others. The intrinsic nonlinear properties of plasmas as dispersive media are known to play a crucial role, leading to various types of collective excitations in the form of localized modes (solitary waves, shocks). Plasma fluid models, mimicking Navier-Stokes equation in hydrodynamics, can be reduced through standard methods to well-known nonlinear partial differential equations of mathematical physics, such as the celebrated nonlinear Schrödinger (NLS) equation known to govern the envelope dynamics of a modulated wavepacket in dispersive media.

Following the pioneering work of Refs. [1, 2], the NLS equation has subsequently been derived for a variety of electrostatic plasma modes within the fluid plasma formalism. Building up on similar considerations in nonlinear optics, its localized solutions (envelope solitons, breathers) have in fact been associated with freak waves [3–6]. Similar derivations of formally analogous NLS equations (but in different context) have focused on electromagnetic waves in plasmas, modeled by fluid-Maxwell equations [7–9], also proposing a rogue wave related interpretation [9].

If one considers a pair of co-propagating (interacting) wavepackets in plasmas, a particular plasma fluid model leads to a pair of coupled NLS (CNLS) equations, whose coefficients generally depend on the carrier wavenumber(s) of the respective waves. Examples include electron plasma (Langmuir) waves and ion acoustic waves mainly [10–12], amidst other studies that focused mostly on electromagnetic modes [13–19].

A number of works on single NLS equations derived from various plasma fluid models have appeared in the literature, in which soliton, breather, and rogue wave solutions were investigated by using known

analytical forms representing those localized structures. However, analogous investigations of two (or more) nonlinear co-propagating and interacting waves in plasma systems are rather scarce (see the references above). Thus, it is meaningful to derive a pair of coupled NLS equations for the plasma fluid model described above, showcasing the analytical dependence of all relevant coefficients on the carrier wavenumber(s) of the respective waves. It is also meaningful and, in fact, a challenging task to investigate how the modulational instability phenomenon, a universal mechanism responsible for wave localization, may occur such electrostatic wave pairs.

Although the derived CNLS equations obey a general form, the dependence of the dispersion, self-nonlinearity and cross-modulation coefficients on the wavenumbers of the respective waves (and, in fact, on the plasma parameters) is unique for each considered plasma fluid model. An important common feature in is that, assuming arbitrary carrier wavenumber (values), these coefficients do not exhibit any obvious symmetry, thus rendering the CNLS equations asymmetric. These general CNLS equations may formally reduce, in certain special case, to known CNLS models such as the Manakov model [20, 21] which is long known to be integrable.

Various plasma related experimental studies have actually focused on the emergence of envelope solitons [22] and breathers [23]. It is remarkable that the observed soliton and breather waveforms can be investigated within the framework of the NLS equation and its already known analytical solutions. Recall, at this point, that CNLS equations and their known solutions have been employed in the description of solitons and breathers in water waves, exhibiting good agreement with experimental observations [24]. In the light of the above considerations, a meticulous study of the modulational instability mechanism associated with energy localization in plasmas may be worth investigating in laboratory realizations of coupled electrostatic waveforms, by means of CNLS (systems of) equation whose coefficients encompass all of the intrinsic plasma wave dynamics.

In this paper, a pair of CNLS equations is derived from a plasma model comprising of a cold inertial ion fluid evolving against a thermalized electron background that follows the Maxwell-Boltzmann distribution, using a standard multiple scale approach (the Newell method). The coefficients of the CNLS equations are provided as functions of the wavenumbers of the two interacting waves and the coefficients of the (approximation of) the Maxwell-Boltzmann distribution. The values of these coefficients for arbitrary carrier wavenumbers of the two waves render the system generally asymmetric. A compatibility condition is also derived, in the form of a fourth degree polynomial in the frequency of the perturbation. The modulational instability (MI) in the system is then investigated with respect to the wavenumber (values) of the two carrier waves and the wavenumber of the perturbation, by numerically obtaining the roots of the compatibility condition and by calculating the magnitude of the associated instability growth rate.

This Article is laid out as follows: the following Section 2 introduces the plasma fluid model equations, from which the pair of CNLS equations are derived using the multiple-scale perturbation method. In Section 3, we undertake an analytical study of the modulational stability analysis of plane wave solutions of the CNLS equations. A detailed parametric analysis of modulational instability occurrence is carried out, based on a numerical calculation of the growth rate numerically, in Section 4. Our main results are summarized in the concluding Section 5.

II. PLASMA FLUID MODEL AND REDUCTION TO CNLS EQUATIONS

A. Model equations and normalization

A one-dimensional (1D), non-magnetized plasma model is considered for electrostatic excitations, consisting of a cold inertial ion fluid of density $n_i = n$ and velocity $u_i = u$, evolving against a thermalized electron background. The electron component follows the Maxwell-Boltzmann distribution, hence its (normalized) density n_e is given by

$$n_e = e^\phi \simeq 1 + c_1\phi + c_2\phi^2 + c_3\phi^3, \quad (1)$$

where a Mc Laurin series expansion in powers of the electrostatic potential ϕ was considered in the last step, for $|\phi| \ll 1$. The constant coefficients for the Maxwell-Boltzmann distribution are $c_1 = 2c_2 = 6c_3 = 1$.

That plasma fluid model comprises the following continuity, momentum and Poisson equation(s)

$$\frac{\partial n}{\partial t} + \frac{\partial(nu)}{\partial x} = 0, \quad \frac{\partial u}{\partial t} + u \frac{\partial u}{\partial x} = -\frac{\partial \phi}{\partial x}, \quad \frac{\partial^2 \phi}{\partial x^2} \simeq 1 - n + c_1 \phi + c_2 \phi^2 + c_3 \phi^3, \quad (2)$$

respectively, where n , u , and ϕ are functions of space x and time t .

The above equations (1) and (2) are given in normalized units. Specifically, the space and time variables x and t are normalized to the inverse ion plasma frequency ω_{pi}^{-1} and to the Debye screening length λ_D , respectively, with

$$\lambda_D = \left(\frac{\varepsilon_0 k_B T_e}{z_i n_{i0} e^2} \right)^{1/2}, \quad \text{and} \quad \omega_{pi} = \left[\frac{n_{0,i} (z_i e)^2}{\varepsilon_0 m_i} \right]^{1/2}. \quad (3)$$

The number density variable(s) of ions n and electrons n_e are normalized to their respective equilibrium values $n_{i,0}$ and $n_{e,0} = z_i n_{i,0}$, the ion velocity u is normalized to $c_s = \lambda_D \omega_{pi} = \left(\frac{z_i k_B T_e}{m_e} \right)^{1/2}$, i.e. essentially the (ion-acoustic) sound speed. Finally, the electrostatic potential is normalized to $k_B T_e / e$. Adopting a standard notation, the symbols ε_0 , k_B , T_e , e , m_i , z_i appearing in the latter expressions denote respectively the dielectric permittivity in vacuum, the Boltzmann's constant, the (absolute) electron temperature, the electron charge, the ion mass, and the degree of ionization ($z_i = q_i / e$, where q_i is the ion charge).

B. Derivation of the coupled CNLS equations

We have undertaken a long algebraic procedure, adopting a multiple scales perturbation technique, to derive a system of evolution equations for the amplitudes (envelopes) describing a pair of (co-propagating) electrostatic wavepackets. Details on the methodology adopted are reported in the Appendix. For clarity in presentation, only the main steps are presented in the following.

We introduce fast and slow variables, viz. $x_n = \varepsilon^n x$ and $t_n = \varepsilon^n t$ (for $n = 0, 1, 2, 3, \dots$), where $\varepsilon \ll 1$ is a small real constant. On the other hand, the dependent variables n , u , and ϕ are expanded in powers of ε , around the equilibrium state, as

$$n = 1 + \varepsilon n_1 + \varepsilon^2 n_2 + \varepsilon^3 n_3 + \dots, \quad u = \varepsilon u_1 + \varepsilon^2 u_2 + \varepsilon^3 u_3 + \dots, \quad \phi = \varepsilon \phi_1 + \varepsilon^2 \phi_2 + \varepsilon^3 \phi_3 + \dots. \quad (4)$$

Substituting the above expansions into Eqs. (2), one obtains various sets of equations at different orders in ε . We have proceeded up to order ε^3 .

The first-order ($\sim \varepsilon^1$) equations are solved by introducing the following *Ansatz*:

$$S_1 = S_{1,1}^{(-1)} e^{-i\theta_1} + S_{1,1}^{(1)} e^{+i\theta_1} + S_{1,2}^{(-1)} e^{-i\theta_2} + S_{1,2}^{(1)} e^{+i\theta_2}, \quad (5)$$

where $S_1 = \{n_1, u_1, \phi_1\}$ is the state vector (triplet) to 1st order, and the phases are given by $\theta_j = k_j x - \omega_j t$, with k_j and ω_j being the wavevector and the corresponding frequency of the j -th wave; note that reality of the state variables imposes $S_{1,j}^{(-1)} = (S_{1,j}^{(1)})^*$ (for $j = 1, 2$), where the star (*) denotes the complex conjugate. A compatibility condition leads to a (common) linear frequency dispersion relation, to be obeyed by both wavepackets ($j = 1, 2$). The angular frequency for the j -th wave and the corresponding group velocity read:

$$\omega_j = \frac{k_j}{\sqrt{k_j^2 + c_1}}, \quad v_{g,j} = \frac{\partial \omega_j}{\partial k_j} = \frac{c_1}{(k_j^2 + c_1)^{3/2}}. \quad (6)$$

(Note that only the positive branch for both ω and k is considered.) In the following, both the wavenumbers k_j and the corresponding dispersion frequency ω_j will appear in the derived mathematical expressions. This is done only for convenience and for ease in the presentation and wherever it occurs, it is implied that ω_j is provided by Eq. (6) as a function of k_j .

The first-order equations may now be solved in terms of the variables $\phi_{1,j}^{(1)} = \Psi_j$ (for $j = 1, 2$), to yield

$$n_{1,j}^{(1)} = \left(\frac{k_j}{\omega_j} \right)^2 \Psi_j, \quad u_{1,j}^{(1)} = \frac{k_j}{\omega_j} \Psi_j, \quad \phi_{1,j}^{(1)} = \Psi_j, \quad (7)$$

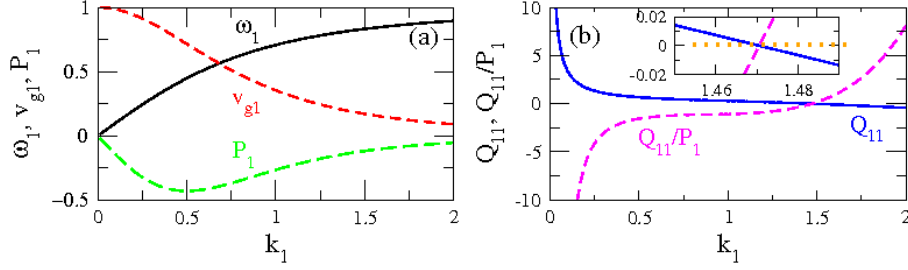


FIG. 1. (a) The linear frequency dispersion ω_1 , the group velocity $v_{g,1}$, and the dispersion coefficient P_1 are depicted as functions of the wavenumber k_1 . Note that P_1 is always negative (in the cold fluid model). (b) The nonlinearity coefficient Q_{11} and the ratio Q_{11}/P_1 are depicted as functions of the wavenumber k_1 . Note that both Q_{11} and Q_{11}/P_1 can be either positive or negative, and that they have a root at $k_1 = 1.47$ as was expected.

where we defined the function(s) Ψ_j (for the j - wave), denoting the leading-order electrostatic amplitude disturbance (amplitudes). These will be our main state variables in the modulational analysis to follow.

An interesting constraint arises in second order ($\sim \varepsilon^2$), where suppression of secular terms imposes the condition(s)

$$\frac{\partial \Psi_j}{\partial t_1} = -v_{g,j} \frac{\partial \Psi_j}{\partial x_1} \quad (8)$$

(for $j = 1, 2$). Recall that the group velocity was defined earlier, based on the dispersion relation found earlier. Physically speaking, this means that the wavepacket amplitudes move at the group velocity, as expected. This is a well known result, related with the so called Newell technique in nonlinear optics; see e.g. in Ref. [25].

Once the above compatibility condition has been applied, the equations arising in second order can be solved, for various harmonic amplitudes. One thus obtains solutions (for the two wavepackets) in the form of a superposition of first and second harmonics and combinations (i.e. sum and difference) thereof. (Details are provided in the Appendix.)

Proceeding to third order ($\sim \varepsilon^3$), once again, a pair of compatibility conditions must be imposed for annihilation of secular terms. One is thus led to a pair of coupled NLS equations in the form

$$i \left(\frac{\partial \Psi_1}{\partial t_2} + v_{g,1} \frac{\partial \Psi_1}{\partial x_2} \right) + P_1 \frac{\partial^2 \Psi_1}{\partial x_1^2} + (Q_{11} |\Psi_1|^2 + Q_{12} |\Psi_2|^2) \Psi_1 = 0, \quad (9)$$

$$i \left(\frac{\partial \Psi_2}{\partial t_2} + v_{g,2} \frac{\partial \Psi_2}{\partial x_2} \right) + P_2 \frac{\partial^2 \Psi_2}{\partial x_1^2} + (Q_{21} |\Psi_1|^2 + Q_{22} |\Psi_2|^2) \Psi_2 = 0, \quad (10)$$

where

$$P_j = -\frac{3}{2} c_1 \frac{k_j}{(k_j^2 + c_1)^{5/2}}, \quad (j = 1, 2) \quad (11)$$

are the dispersion coefficients and

$$Q_{jj} = \frac{\omega_j}{2k_j^2} \tilde{Q}_{jj}, \quad Q_{12} = \frac{\omega_1}{2k_1^2} \tilde{Q}_{12}, \quad Q_{21} = \frac{\omega_2}{2k_2^2} \tilde{Q}_{21} \quad (12)$$

are the self modulation and cross-coupling coefficients, respectively. (Expressions for the tilded quantities are provided in the Appendix.) Note that Q_{12} and Q_{21} exchange expressions, upon permuting k_1 and k_2 (and ω_1 and ω_2), as intuitively expected, upon a simple symmetry argument.

As we shall see below, the coefficients P_j and Q_{ij} in Eqs. (9) and (10) do not exhibit any particular symmetry for arbitrary values of the wavenumbers k_1 and k_2 , as e.g. in the famous Manakov model [20] which was proven to be completely integrable. During the last decades, other different variants of CNLS systems of equations were investigated in various contexts and were proven to be integrable [26–29]. Note that our CNLS system recovers all of these systems in appropriate limits. However, as stated above, it is a-symmetric in its general form.

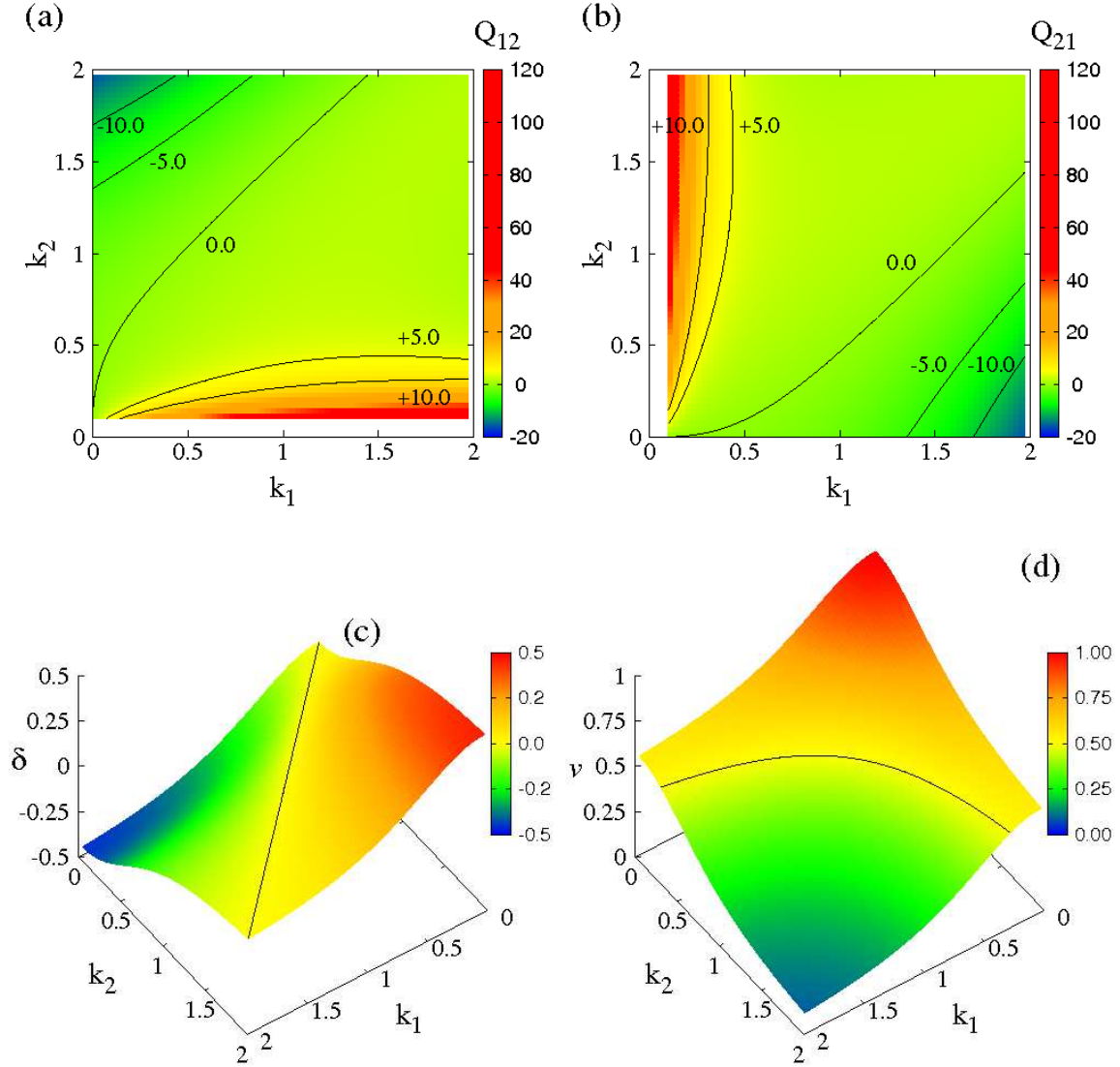


FIG. 2. The nonlinear coupling coefficient Q_{12} (a) and Q_{21} (b) are depicted as functions of the respective wavenumber(s) of the two co-propagating carrier waves, k_1 and k_2 . The black curves in (a) and (b) represent five contours at the values $(0, \pm 5, \pm 10)$ of Q_{12} and Q_{21} , respectively, as shown on the figures. In the white areas in (a) and (b), the coupling coefficients Q_{12} (for low k_2) and Q_{21} (for low k_1), respectively, assume very high values that have been omitted for clarity. The half-difference δ (c) and the half-sum V (d) of the group velocities are also shown on the $k_1 - k_2$ plane. The black curves on the surface of (c) and (d) are contours at $\delta = 0$ and $V = 0.5$, respectively.

In Fig. 1(a) the frequency dispersion ω_1 , the group velocity v_{g1} , and the dispersion coefficient P_1 are all plotted as a function of the wavenumber of the first carrier wave k_1 . The corresponding nonlinearity coefficient Q_{11} and the ratio Q_{11}/P_1 are shown also as a function of k_1 in Fig. 1(b). The corresponding quantities for the second carrier wave (i.e., ω_2 , v_{g2} , Q_{22} , etc.) as functions of the carrier wavenumber k_2 have exactly the same form (upon shifting k_1 to k_2). Note that, for the cold-ion fluid model considered here, the dispersion coefficients P_j ($j = 1, 2$) are both negative for any k_j , in fact converging asymptotically to zero from below for large k_j . (This fact is expected to change if one considers a warm ion fluid.) On the other hand, the nonlinearity coefficients Q_{jj} can be either positive or negative, depending on the value of k_j : they both exhibit one real root at $k_j = 1.47$ as expected from previous works [2] (and refs. therein), so that $Q_{jj} > 0$ for $k_j < 1.47$ and $Q_{jj} < 0$ otherwise.

The coupling coefficients Q_{12} and Q_{21} given in Eqs. (12) clearly depend on both k_1 and k_2 , and they

exhibit a reflection symmetry around $k_1 = k_2$, as intuitively expected. Two-dimensional maps for Q_{12} and Q_{21} on the $k_1 - k_2$ wavenumber plane are shown in Figs. 2(a) and 2(b), respectively. The half-difference and the half-sum of the group velocities δ and V , respectively, are shown on the $k_1 - k_2$ plane in Figs. 2(c) and 2(d).

C. Transformation to the regular CNLS equations form

Equations (A35) and (A36) can be transformed to the most common form of CNLS equations with a change of independent variables, followed by a transformation. Let us introduce the new variables ξ and τ through (drop the subscripts in x and t)

$$\xi = x - vt, \quad \tau = t, \quad (13)$$

where $v = (v_{g,1} + v_{g,2})/2$, is the half-sum of the group velocities $v_{g,1}$ and $v_{g,2}$. Using v and the half-difference of the group velocities $\delta = (v_{g,1} - v_{g,2})/2$ we have that

$$v_{g,1} = v + \delta, \quad v_{g,2} = v - \delta. \quad (14)$$

By applying the change of variables to Eqs. (A35) and (A36) we get

$$i \left(\frac{\partial \Psi_1}{\partial \tau} + \delta \frac{\partial \Psi_1}{\partial \xi} \right) + P_1 \frac{\partial^2 \Psi_1}{\partial \xi^2} + \{Q_{11}|\Psi_1|^2 + Q_{12}|\Psi_2|^2\} \Psi_1 = 0, \quad (15)$$

$$i \left(\frac{\partial \Psi_2}{\partial \tau} - \delta \frac{\partial \Psi_2}{\partial \xi} \right) + P_2 \frac{\partial^2 \Psi_2}{\partial \xi^2} + \{Q_{21}|\Psi_1|^2 + Q_{22}|\Psi_2|^2\} \Psi_2 = 0. \quad (16)$$

In writing the latter equations, it is implicitly understood that the differentiations involved in the dispersive terms are with respect to the variable ξ_1 , while the higher-order differentiation in the beginning of the LHS are with respect to ξ_2 . The subscripts are nonetheless omitted, for simplicity, as they will not affect the final result. Next, we apply to Eqs. (15) and (16) the following transformation

$$\Psi_1 = \bar{\Psi}_1 \exp \left[i \left(\frac{\delta^2}{4P_1} \tau - \frac{\delta}{2P_1} \xi \right) \right], \quad (17)$$

$$\Psi_2 = \bar{\Psi}_2 \exp \left[i \left(\frac{\delta^2}{4P_2} \tau + \frac{\delta}{2P_2} \xi \right) \right], \quad (18)$$

where $\bar{\Psi}_1$ and $\bar{\Psi}_2$ are complex functions of the new variables ξ and τ , to get after some straightforward algebra:

$$i \frac{\partial \bar{\Psi}_1}{\partial \tau} + P_1 \frac{\partial^2 \bar{\Psi}_1}{\partial \xi^2} + \{Q_{11}|\bar{\Psi}_1|^2 + Q_{12}|\bar{\Psi}_2|^2\} \bar{\Psi}_1 = 0, \quad (19)$$

$$i \frac{\partial \bar{\Psi}_2}{\partial \tau} + P_2 \frac{\partial^2 \bar{\Psi}_2}{\partial \xi^2} + \{Q_{21}|\bar{\Psi}_1|^2 + Q_{22}|\bar{\Psi}_2|^2\} \bar{\Psi}_2 = 0. \quad (20)$$

Formally equivalent CNLS equations to those in Eqs. (9)-(10), or to those in (19)-(20), have been obtained earlier, for different plasma fluid models [10, 11, 13–16, 18, 19], as mentioned in the introduction, and also in several other physical contexts, e.g., in pulse propagation in water waves [24], in deep water wave propagation [30], in the study of asymmetric coupled wavefunctions [31], in soliton propagation in left-handed transmission lines [32], in left-handed metamaterials [33], in the study of pulses of different polarizations in anisotropic dispersive media [34], in pulse propagation in optical nonlinear media [35], and in randomly birefringent optical fibers [36], among others. Theoretical and computational studies of envelope solitons in coupled NLS models have been presented in Ref. [37], while a brief overview of various localized solutions in the Manakov model is given in Ref. [38]. Note that when $P_j = 1$ and $Q_{11} = Q_{21} = -Q_{22} = -Q_{12}$ our system reduces to the one treated in Refs. [39, 40].

a. *An alternative form of the CNLS system.* It is worth pointing out that the number of nontrivial parameters in the CNLS equations Eqs. (19) and (20) can be reduced by rescaling the dependent and the independent variables. One may follow the procedure in [32, 41] by assuming $Q_{11}, Q_{22} > 0$ and $P_1 \neq 0$, and simultaneously applying the transformations

$$\hat{\Psi}_j = \bar{\Psi}_j \sqrt{Q_{jj}}, \quad \zeta = \xi / \sqrt{|P_1|}, \quad (21)$$

to Eqs. (19) and (20). One thus obtains

$$i \frac{\partial \hat{\Psi}_1}{\partial \tau} + s \frac{\partial^2 \hat{\Psi}_1}{\partial \zeta^2} + \left\{ |\hat{\Psi}_1|^2 + \mu_{12} |\hat{\Psi}_2|^2 \right\} \hat{\Psi}_1 = 0, \quad (22)$$

$$i \frac{\partial \hat{\Psi}_2}{\partial \tau} + p \frac{\partial^2 \hat{\Psi}_2}{\partial \zeta^2} + \left\{ |\hat{\Psi}_2|^2 + \mu_{21} |\hat{\Psi}_1|^2 \right\} \hat{\Psi}_2 = 0, \quad (23)$$

where

$$\mu_{12} = \frac{Q_{12}}{Q_{22}}, \quad \mu_{21} = \frac{Q_{21}}{Q_{11}}, \quad p = \frac{P_2}{|P_1|}, \quad s = \frac{P_1}{|P_1|} = \pm 1 \quad (24)$$

and the number of nontrivial parameters has thus been reduced to three [32, 41], or rather four (including s , i.e. the sign of P_1). Do not forget that this conclusion comes under the assumption that the dispersion coefficient P_1 is finite, i.e. non-zero, and that the nonlinearity coefficients Q_{11} and Q_{22} are all positive. Recall that $P_1 < 0$, actually, in the cold-ion model considered here, hence $s = -1$ here.

III. MODULATIONAL STABILITY ANALYSIS: ANALYTICAL FRAMEWORK

The modulational stability analysis for two co-propagating wavepackets in the plasma described by the fluid equations (2) may now be performed, relying on the CNLS equations (15) and (16) following the procedure of Refs. [19, 31]. For this purpose we first seek a plane-wave solution of the form

$$\Psi_j = \Psi_{j,0} e^{i\tilde{\omega}_j \tau}, \quad (25)$$

where $\Psi_{j,0}$ ($j = 1, 2$) is a constant real amplitude and $\tilde{\omega}_j$ is a real frequency correction to be determined.

By inserting Eq. (25) into Eqs. (15) and (16), we get

$$\tilde{\omega}_1 = Q_{11} \Psi_{1,0}^2 + Q_{12} \Psi_{2,0}^2, \quad \text{and} \quad \tilde{\omega}_2 = Q_{21} \Psi_{1,0}^2 + Q_{22} \Psi_{2,0}^2. \quad (26)$$

Eq. (25), with the frequency correction(s) given by Eq. (26), provide a linear coupled-mode solution of the CNLS system (a coupled Stokes wave pair, actually, in the hydrodynamic picture) wherein the propagation of waves is governed by Eqs. (15) and (16). In order to address the stability of the above plane-wave solutions against a small perturbation, we take

$$\Psi_j = (\Psi_{j,0} + \varepsilon_j) e^{i\tilde{\omega}_j \tau}, \quad (27)$$

where ε_j represents a complex perturbation on the amplitudes of the two waves ($|\varepsilon_j| \ll \Psi_{j,0}$). By inserting the perturbed amplitudes Ψ_j into Eqs. (15) and (16), we obtain

$$i \left(\frac{\partial \varepsilon_1}{\partial \tau} + \delta \frac{\partial \varepsilon_1}{\partial \xi} \right) + P_1 \frac{\partial^2 \varepsilon_1}{\partial \xi^2} + Q_{11} \Psi_{1,0}^2 (\varepsilon_1 + \varepsilon_1^*) + Q_{12} \Psi_{1,0} \Psi_{2,0} (\varepsilon_2 + \varepsilon_2^*) = 0, \quad (28)$$

$$i \left(\frac{\partial \varepsilon_2}{\partial \tau} - \delta \frac{\partial \varepsilon_2}{\partial \xi} \right) + P_2 \frac{\partial^2 \varepsilon_2}{\partial \xi^2} + Q_{22} \Psi_{2,0}^2 (\varepsilon_2 + \varepsilon_2^*) + Q_{21} \Psi_{2,0} \Psi_{1,0} (\varepsilon_1 + \varepsilon_1^*) = 0. \quad (29)$$

Setting $\varepsilon_j = g_j + ih_j$, where g_j and h_j are real functions, then subsequently substituting into Eqs. (28) and (29) and eventually eliminating the imaginary parts h_j from the resulting equations, we obtain for the real parts:

$$\left\{ \left(\frac{\partial}{\partial \tau} + \delta \frac{\partial}{\partial \xi} \right)^2 + P_1 \left(P_1 \frac{\partial^2}{\partial \xi^2} + 2Q_{11} \Psi_{1,0}^2 \right) \frac{\partial^2}{\partial \xi^2} \right\} g_1 + 2P_1 Q_{12} \Psi_{2,0} \Psi_{1,0} \frac{\partial^2}{\partial \xi^2} g_2 = 0, \quad (30)$$

$$\left\{ \left(\frac{\partial}{\partial \tau} - \delta \frac{\partial}{\partial \xi} \right)^2 + P_2 \left(P_2 \frac{\partial^2}{\partial \xi^2} + 2Q_{22} \Psi_{2,0}^2 \right) \frac{\partial^2}{\partial \xi^2} \right\} g_2 + 2P_2 Q_{21} \Psi_{1,0} \Psi_{2,0} \frac{\partial^2}{\partial \xi^2} g_1 = 0. \quad (31)$$

Eventually, by setting (i.e. considering harmonic amplitude perturbations)

$$g_j = g_{j,0} e^{i(K\xi - \Omega\tau)} + c.c., \quad (32)$$

where *c.c.* denotes the complex conjugate, and then substituting into the earlier equations, we obtain after some algebra a *compatibility condition*

$$[(\Omega - K\delta)^2 - \Omega_1^2] [(\Omega + K\delta)^2 - \Omega_2^2] = \Omega_c^4, \quad (33)$$

where

$$\Omega_1^2 = P_1 K^2 (P_1 K^2 - 2Q_{11} \Psi_{1,0}^2), \quad \Omega_2^2 = P_2 K^2 (P_2 K^2 - 2Q_{22} \Psi_{2,0}^2), \quad \Omega_c^4 = 4P_1 P_2 Q_{12} Q_{21} \Psi_{1,0}^2 \Psi_{2,0}^2 K^4. \quad (34)$$

This is essentially a dispersion relation for the amplitude perturbation considered above. So long as *all* solutions for Ω are real, the amplitude perturbation will be stable to external disturbances, e.g. noise. Conversely, for instability to set in, at least one (of the four) solutions of the quartic polynomial Eq. (33) in Ω should have a positive imaginary part.

The growth rate of the modulational instability is then defined as

$$\Gamma = \max\{Im(\Omega)\}, \quad (35)$$

i.e. is given by the maximum value of the imaginary part of the solution. (Note that either two complex conjugate solutions will exist, or otherwise four – i.e. two pairs of complex conjugates – in which case the maximum value will dominate. Negative values of the imaginary part will lead to decaying modes.)

Relevance with Space plasmas. Evidence of MI processes in space was found since the very early stages of space missions [42–45]. On several occasions, the theory of MI is capable of explaining the generation of modulated wave envelopes commonly observed in space plasmas, as well as solitary waves and freak or rogue waves. Such processes, in particular, can explain the detection of electric field wave envelopes observed in the terrestrial auroral zone [42, 43]. In Ref. [42], the authors reported direct evidence of nearly 100% electric field amplitude modulation of Langmuir waves (see their Figure 2) observed in the auroral ionosphere. These data are consistent with a transverse MI, whose characteristic frequencies are near the observed modulational frequencies (obtained by independent measurements). In Ref. [43], several hundreds of large amplitude and narrow-band modulated Langmuir waves (observed by Freja satellite and SCIFER sounding rocket in the terrestrial auroral zone) were used to estimate their modulation frequencies. It was shown that lower hybrid waves in the cold electrostatic limit can produce the estimated modulation frequencies (i.e., several tens of kilohertz). In Ref. [44], the author analyzed a model of coupled mode equations describing plasma wave turbulence in the strongly magnetized pair plasma of a pulsar polar cap. Numerical solutions of the model equations reveal the development of turbulence, whose onset involves a secondary wave-wave (modulational) instability. In Ref. [45], the possibility of generating large-amplitude and short-lived wavepackets from small-amplitude initial perturbations in various plasmas is discussed. The author presents a figure (Figure 1 in his article) for the hour averages of the magnetic field strength in the heliosheath as a function of time, in which the magnitude of the field exhibits many spike-like dips (magnetic holes) which are characterized as freak plasma waves. The author shows that for a particular wave mode, the ion-sound wave in plasma with negative ions described by Gardner equation, a modulationally unstable initial condition leads through MI to the generation of freak or rogue ion-acoustic waves. From the discussion of these works it can be inferred that the mechanism of the MI in various space plasmas is very important and relevant for the generation of modulated wavepackets (envelops) as well as large amplitude solitary waves (freak or rogue waves), among others, which have been observed by space missions. In other words, the generation of these structures seem to be a consequence of MI processes which may occur frequently in plasmas.

IV. MODULATIONAL INSTABILITY: PARAMETRIC ANALYSIS BASED ON NUMERICAL RESULTS

We have computed the growth rate Γ numerically, by finding the roots of the polynomial in Ω based on Eq. (33), and subsequently identifying the one with the highest imaginary part. That highest imaginary

part was then plotted as a function of the wavenumber of the perturbation K and the wavenumber of the second carrier wave k_2 , considering three different values of k_1 and – independently – for two different pairs of values of $A_{1,0}$ and $A_{2,0}$.

In Figs. 3(a), (b), (c) and (d) (for equal amplitudes, $A_{1,0} = A_{2,0} = 0.15$), the four values of the carrier wavenumber k_1 are respectively 0.1, 0.4, 0.7 and 1.6. (Note that the first three were chosen in the modulationally stable region $k_1 < 1.47$, whereas the latter was chosen from the intrinsically unstable range $k_1 > 1.47$.) The figures reveal in all cases shown a rather complex instability pattern. The analogous patterns for $A_{1,0} = 0.0707$ and $A_{2,0} = 0.2$, shown in Figs. 4, reveal that the growth rate is generally lower in this case (for unequal amplitudes $A_{1,0}$ and $A_{2,0}$) while at the same time the K intervals (“windows”) of instability are narrower. Note that the two pairs of amplitudes were chosen so that the norm $A_{1,0}^2 + A_{2,0}^2$ (qualitatively representing the total electrostatic energy injected in the system) remains the same. For the values of k_1 and k_2 used to obtained the results in the first three panels (a)-(c) of both Figs. 3 and 4, the decoupled Eqs. (15) and (16) resulting by setting $Q_{12} = Q_{21} = 0$ are both stable against periodic perturbations since $P_j Q_{jj} < 0$. (Recall that P_j is always negative in the considered model and that Q_{jj} is positive for $k_j < 1.47$.) In contrast to this picture, the fourth panel (d), in both of these figures, corresponds to the unstable case $k_1 > 1.47$, for the first wave. On the other hand, the second wavepacket may either be (independently) stable (for $k_2 < 1.47$) or unstable (for $k_2 > 1.47$), i.e. in the absence of its sister wave 1. Implicitly, all four combinations — say $\text{sgn}(P_j Q_{jj}) \in (+/+, +/-, -/+, -/-)$ — in the combined stability profile of the wave pair have thus been taken into consideration (albeit with arbitrary, sample parameter values).

Significant qualitative conclusions may be drawn based on critical inspection of our indicative numerical plots. If one draws a vertical line at $k_2 = 1.47$, in any of the (8) plots presented in Figs. 3 and 4, the area on the left (right) of that vertical line will correspond to a region where the 2nd wave is intrinsically unstable (stable). As expected, in panels (a)-(c) of both of Figs. 3 and 4, the map-profile is darker (blue color is dominant) on the left half of the plots: this reveals that, when both waves – in the absence of each other’s sister wave – are modulationally stable, their coupling may lead to the system being destabilized, yet this is rather limited to regions of large perturbation wavenumber K (see the small islands top left, in Figures 3(c), 4(a) and 4(c)). The resulting instability (due to the nonlinear coupling between two otherwise stable wavepackets) is more intense in the case of unequal amplitudes: cf. 4(a) with 3(a)), for strong K and low k_2 .

On the other hand, it is interesting to observe the last sub-panel (d) in either of Figs. 3 and 4. In this one, one of the waves (wave 1) is intrinsically unstable. Therefore, in the right half of sub-panels 3(d) and 4(d) (were both k_1 and k_2 are above 1.47), both waves are modulationally unstable (independently from one another). Still, somehow counter-intuitively, it appears that the coupling results in them being stabilized somehow, for large K (note the blue-colored stability region in the top right quadrant in both these plots). However, by comparing the growth rate Γ in Figs. 3(d) and 4(d) with the corresponding rates Γ_1 and Γ_2 of the two single NLS equations resulting from the decoupled CNLS system, we observe that Γ is always larger in magnitude and and that the instability interval in K is much larger than the corresponding ones of Γ_1 and Γ_2 . An illustrative example of this situation can be seen in Fig. 5(b) below.

On the other hand, the left half of these sub-plots corresponds to a situation where one (1) of the waves (2) is stable, while the other one (1) is unstable. As seen in the other plots too, this combination leads to an unstable pair of wavepackets.

As discussed above, when either one of the k_j s or both k_j s is (are) greater than 1.47, the system of the CNLS Eqs. (15) and (16) is again modulationally unstable for K values within certain intervals (instability windows). An illustrative example is shown in Fig. 5 for $k_1 = 1.48$ and $k_2 = 1$ (a), $k_2 = 1.5$ (b), and $k_2 = 2$ (c). In this figure, the growth rate Γ of the system of Eqs. (15)-(16) is compared with the growth rates Γ_1 and Γ_2 , obtained respectively from the first and second decoupled Eqs. (15) and (16) upon “switching off” the coupling, setting $Q_{ij} = 0$ for $i \neq j$ for a minute — or, more accurately, upon setting $k_2 = 0$ in Eq. (15) and $k_1 = 0$ in Eq. (15). For those decoupled equations, in particular, by using the same modulational instability analysis as it was used in the beginning of this section, we find that the growth rates Γ_1 and Γ_2 are given by the magnitude of the imaginary part of the perturbation frequency Ω obtained from the equations

$$\Omega = +\delta K \pm \Omega_1, \quad \Omega = -\delta K \pm \Omega_2, \quad (36)$$

for the first and the second decoupled NLS equation, respectively. The results shown in Fig. 5 reveal that the growth rate Γ of the system of coupled NLS equations is always much larger that the growth

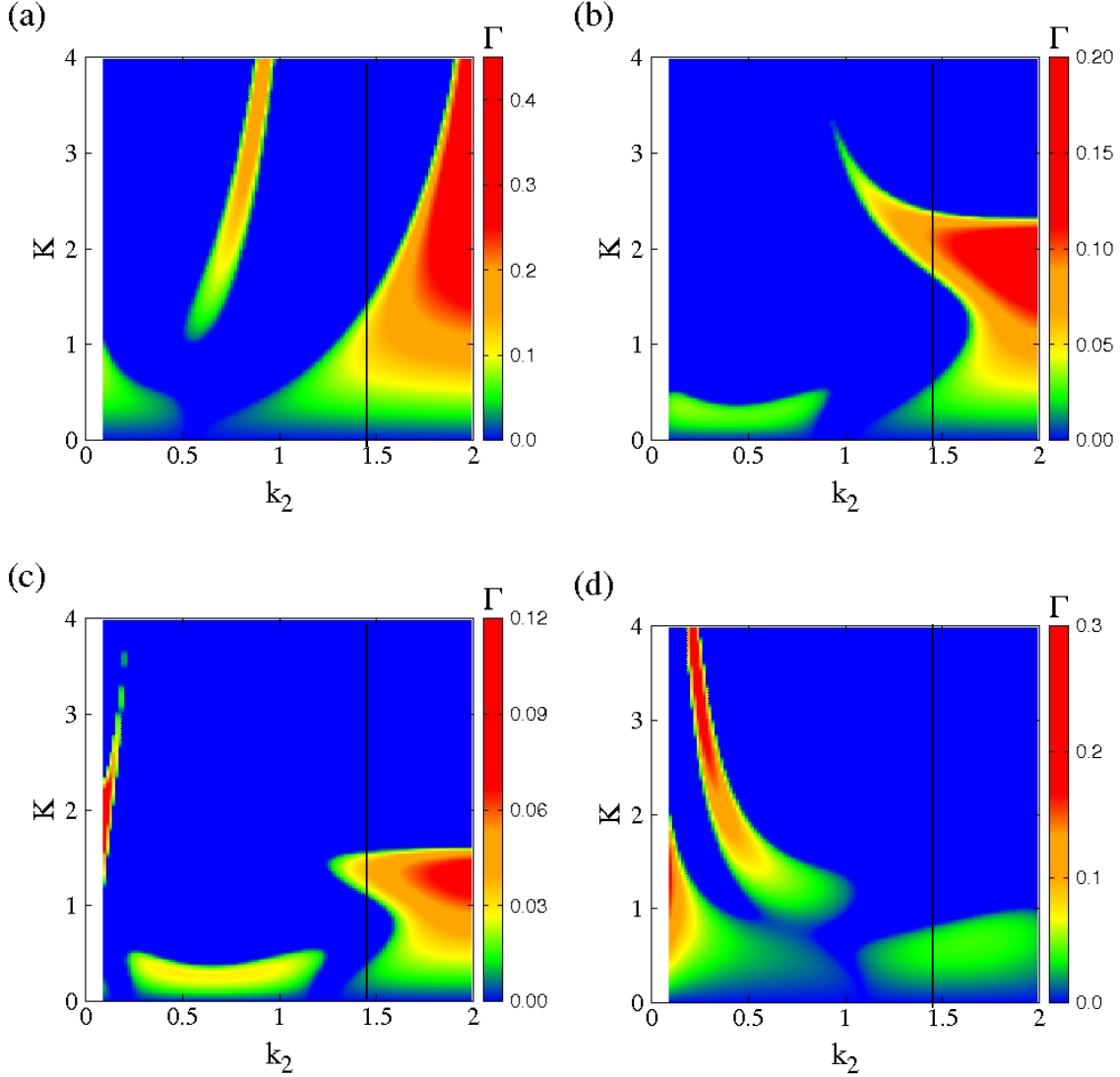


FIG. 3. The growth rate Γ as a function of the wavenumber of the second carrier wave k_2 and the wavenumber of the perturbation K for $A_{1,0} = A_{2,0} = 0.15$, and (a) $k_1 = 0.1$, (b) $k_1 = 0.4$, (c) $k_1 = 0.7$, (d) $k_1 = 1.6$. The black vertical line is located at $k_2 = 1.47$ and separates areas on the plane with positive (left from the line) and negative (right from the line) Q_{22} .

rates Γ_1 and Γ_2 of the decoupled equations. Moreover, in the CNLS equations, the instability occurs in much larger intervals of the wavenumber of the perturbation K . As a consequence, besides the qualitative effect of the coupling (discussed in the previous paragraph), its *quantitative* impact is dramatic, in that wave-wave coupling results in an increased growth rate and an enhanced instability window.

A. Special case: decoupled second wave, ($Q_{21} = 0$)

In the general case, the choice of a pair of wavenumbers (k_1, k_2) leads generally to different values for Q_{ij} and P_j . As mentioned earlier, the nonlinearity coefficients Q_{jj} change their sign, from positive to negative, as the wavenumber k_j exceeds 1.47. Moreover, as one may have notice from Figs. 2(a) and (b), Q_{12} or Q_{21} (but not both) can become zero on the particular curve on the $k_1 - k_2$ plane. Let us choose a pair of (k_1, k_2) values for which, say Q_{21} is zero. In that case, Eq. (16) is not affected by Eq. (15),

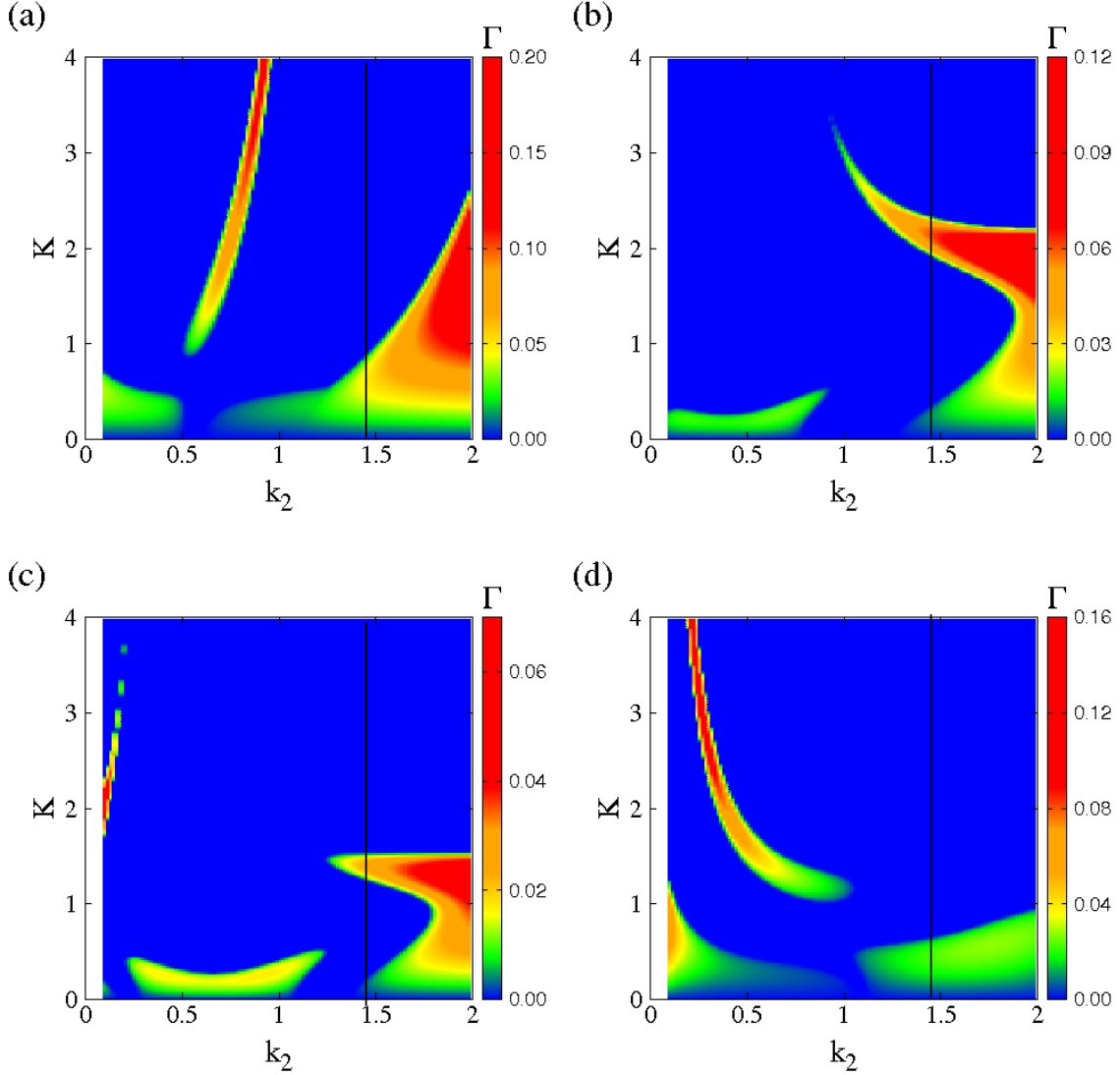


FIG. 4. The growth rate Γ as a function of the wavenumber of the second carrier wave k_2 and the wavenumber of the perturbation K for $A_{1,0} = 0.0707$, $A_{2,0} = 0.2$, and (a) $k_1 = 0.1$, (b) $k_1 = 0.4$, (c) $k_1 = 0.7$, (d) $k_1 = 1.6$. The black vertical line is located at $k_2 = 1.47$ and separates areas on the plane with positive (left from the line) and negative (right from the line) Q_{22} .

although the latter is still affected by the former. In this interesting situation, the perturbation dispersion relation reduces into two independent quadratic equations. Each of them is the dispersion relation for an NLS equation which is uncoupled from the other NLS equation. The roots of the dispersion relation in this case are then the same as those in Eq. (36). Thus, the condition for stability is the same as that for the two decoupled NLS equations, i.e., $P_1 Q_{11} < 0$ and $P_2 Q_{22} < 0$.

In Figs. 6(a) and 6(c), the Q_{ij} s are plotted as a function of k_2 for fixed $k_1 = 0.7$ and 1.5 , respectively. For these parameter values, the coupling coefficient Q_{21} becomes zero at $k_2 \simeq 0.2160$ and 0.9529 , respectively. Subsequently, for the pairs of (k_1, k_2) where $Q_{21} = 0$, i.e., for $(k_1, k_2) = (0.7, 0.2160)$ and $(k_1, k_2) = (1.5, 0.9529)$, the perturbation frequency dispersions are plotted in Figs. 6(b) and 6(d), respectively. In Fig. 6(b) all frequency dispersion branches are real, since both $k_1, k_2 < 1.47$ and $P_1 Q_{11} < 0$, $P_2 Q_{22} < 0$, thus the CNLS system is stable in this case. In Fig. 6(d), however, two of the frequency branches are complex in a particular interval of the perturbation frequency K , since in this case $k_2 < 1.47 < k_1$ and $P_2 Q_{22} < 0 < P_1 Q_{11}$. The branch with the positive imaginary part actually

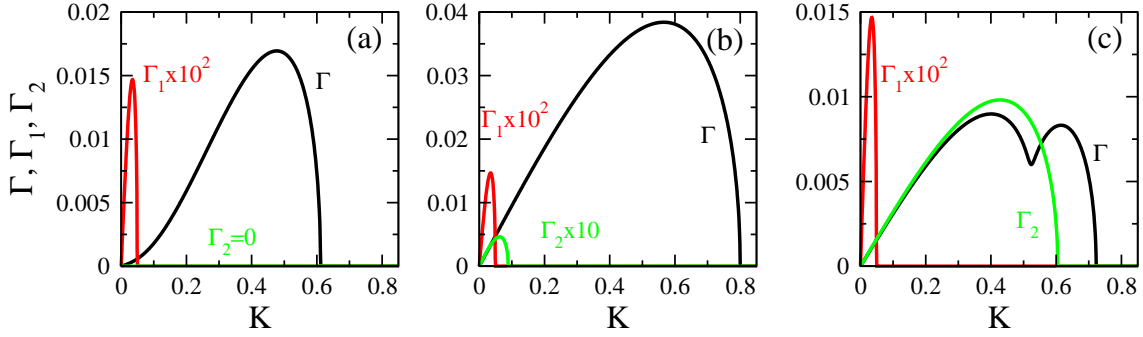


FIG. 5. The growth rate Γ and the the growth rates Γ_1 and Γ_2 of the first and second decoupled Eqs. (15) and (16) as a function of the wavenumber of the perturbation K , for $k_1 = 1.48$ ($Q_{11} < 0$), $A_{1,0} = A_{2,0} = 0.15$, and (a) $k_2 = 1$, (b) $k_2 = 1.5$, (c) $k_2 = 2$.

determines the (in)stability interval in K of the whole system as well as the corresponding growth rate. That imaginary part is plotted in the inset of Fig. 6(d), where we observe that the system is unstable for K in $(0, 0.09)$.

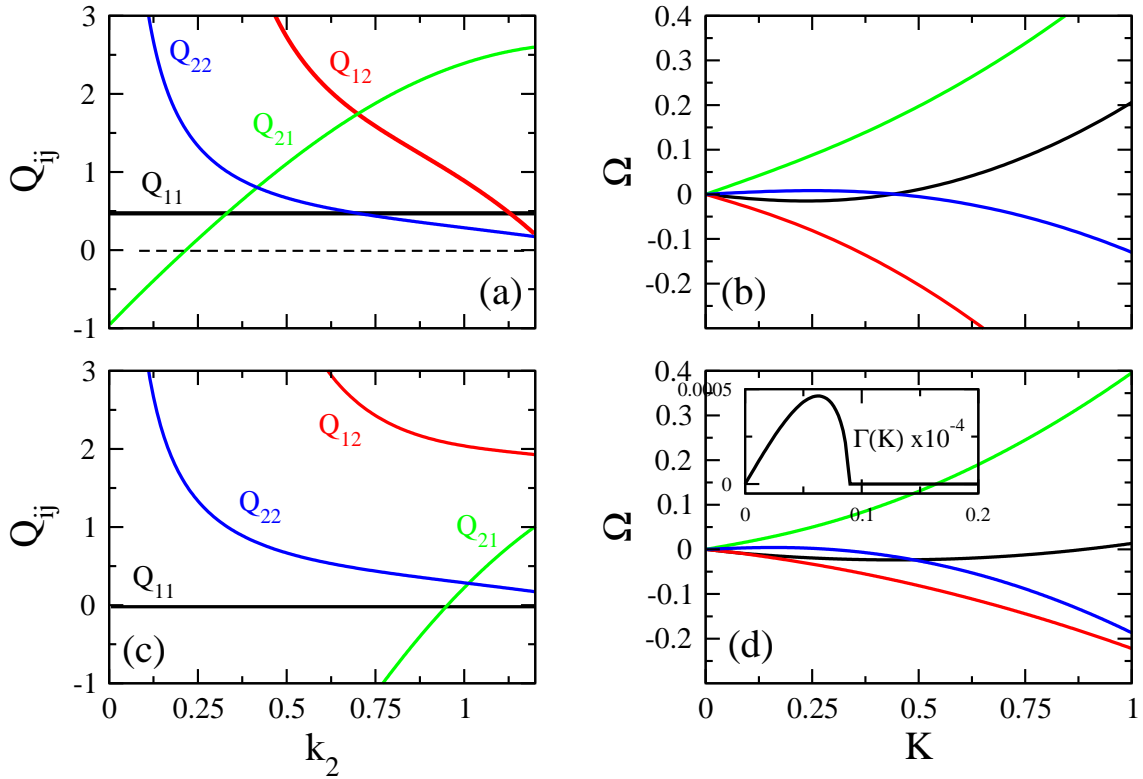


FIG. 6. (a) The coupling and nonlinearity coefficients Q_{ij} ($i, j = 1, 2$) as a function of the wavenumber k_2 of the second carrier wave for $k_1 = 0.7$. The coupling coefficient Q_{21} becomes zero at $k_2 \simeq 0.2160$. (b) The real parts of the perturbation frequency dispersion branches $\Omega = \Omega(K)$ for $k_1 = 0.7$, $k_2 \simeq 0.2160$, and $A_{1,0} = A_{2,0} = 0.15$. The corresponding imaginary parts are zero. (c) As in (a) for $k_1 = 1.5$. Q_{21} becomes zero at $k_2 \simeq 0.9529$. (d) As in (b) for $k_1 = 1.5$, $k_2 \simeq 0.9529$, and $A_{1,0} = A_{2,0} = 0.15$. Inset: The imaginary part of the branch of Ω whose real part is shown in black color, that coincides with the corresponding growth rate Γ .

V. CONCLUSIONS

A set of coupled nonlinear Schrödinger (CNLS) equations was derived for a pair of co-propagating (and interacting) electrostatic wavepackets, governed by a plasma fluid model comprising a cold inertial ion fluid evolving against a thermalized electron background. A multiple-scale technique has been adopted, similar to the well known Newell method in nonlinear optics.

The dispersion, nonlinearity, and coupling coefficients P_j and Q_{ij} ($j = 1, 2$) depend on the carrier wavenumbers k_1 and k_2 (both assumed arbitrary) of the two interacting wavepackets, and in general they differ from each other. The exact mathematical expressions for those coefficients have been analytically obtained, and in fact depend parametrically on the plasma parameters too. Although P_j for the particular model considered here assumes negative values that tend to zero for large k_j , the coefficients Q_{jj} can be either positive or negative, actually becoming zero at $k_j = 1.47$ as discussed earlier. The coupling coefficients Q_{12} and Q_{21} , which depend both on k_1 and k_2 , assume their values from a large interval of positive and negative real numbers. All this prescribes a multifaceted dynamical profile with strong interconnection among the various physical parameters.

A compatibility condition was derived through modulational stability analysis, in the form of a fourth degree polynomial in the frequency of the perturbation. By numerically finding the roots/solutions of the compatibility condition and identifying the one with the largest magnitude of the imaginary part (growth rate), modulationally stable and unstable areas on the $k_2 - K$ plane have been identified. The instability growth rate, mapped on that plane, reveals that modulational instability occurs in areas of the $k_2 - K$ plane (say, for fixed k_1), actually for all four combinations of the sign of the product $P_j Q_{jj}$ of the decoupled equations, i.e. obtained by appropriately selecting the wavenumbers k_1 and k_2 . (Recall that stability imposes $P_j Q_{jj} < 0$ in the single NLS case.)

Modulational instability in fact may occur even if both waves of the decoupled system are stable, since their strong nonlinear coupling may potentially destabilize the system in regions with large perturbation wavenumbers K . The instability that results from the nonlinear coupling between the two wavepackets is more intense in the case of equal amplitudes of the two waves; instability areas also occupy larger areas (“windows”) on the $k_2 - K$ plane in the latter case. When one or both the waves of the decoupled system are unstable, their nonlinear coupling leads again to an unstable pair of wavepackets as shown earlier.

A comparison of the growth rates of the two waves of the decoupled system with that of the waves in the coupled one reveals that the latter is always larger than the former; furthermore, the unstable regions on the $k_2 - K$ plane are larger than those of the waves in the decoupled system.

Note that the modulational instability of the nonlinear co-propagating waves may lead dynamically to the formation of localized electrostatic waveforms of solitonic type (envelope solitons), i.e. essentially components of a vector soliton, while the plasma system remains physically stable. This is a commonly met situation in complex dynamical systems in which a solution loses its stability for a particular parameter set while at the same time a stable solution emerges.

The electron component in this work is assumed to follow the Maxwell-Boltzmann distribution, for simplicity. This “simple” model successfully captures the salient features of modulational interactions between electrostatic plasma wavepackets as regards their envelope dynamics. As a straightforward generalization, our model can be extended to cover a non-Maxwellian particle distribution, such as e.g., a kappa distribution, a common occurrence in Space plasmas. Work in this direction is in progress; preliminary results suggesting a strong dependence of the modulational profile on the electron statistics, were recently presented at a conference [46]. Once completed, this work will form the focus of a forthcoming article.

ACKNOWLEDGEMENTS

Authors IK and NL gratefully acknowledge financial support from Khalifa University of Science and Technology, Abu Dhabi, United Arab Emirates, via the project CIRA-2021-064 (8474000412). IK gratefully acknowledges financial support from KU via the project FSU-2021-012 (8474000352) as well as from KU Space and Planetary Science Center, via grant No. KU-SPSC-8474000336. The contributions (analytical work) by two of us (AJ and GV) to this project were carried out during their respective research visit in 2022, funded by an ADEK (Abu Dhabi Education and Knowledge Council, currently ASPIRE-UAE) AARE (Abu Dhabi Award of Research Excellence) grant (AARE18-179). Hospitality from the

host during those visits is gratefully acknowledged. Author AJ acknowledges support by Tamkeen under the NYU (New York University Abu Dhabi) Research Institute grant CG008. This work was completed while one of us (IK) was a Visiting Researcher at the National and Kapodistrian University of Athens (Greece) during a sabbatical leave; the hospitality of the host is warmly acknowledged.

-
- [1] K. Shimizu and Y. H. Ichikawa, Automodulation of ion oscillation modes in plasma, *J. Phys. Soc. Jpn.* **33** (3), 789–792 (1972); doi: <https://doi.org/10.1143/JPSJ.33.789>.
 - [2] T. Kakutani and N. Sugimoto, Krylov-Bogoliubov-Mitropolsky method for nonlinear wave modulation, *Phys. Fluids* **17**, 1617–1625 (1974); doi: <https://doi.org/10.1063/1.1694942>.
 - [3] I. Kourakis and P. K. Shukla, Exact theory for localized envelope modulated electrostatic wavepackets in space and dusty plasmas, *Nonlinear Process. Geophys.* **12**, 407–423 (2005); doi: <https://doi.org/10.5194/npg-12-407-2005>.
 - [4] N. A. Chowdhury, A. Mannan, M. R. Hossen, and A. A. Mamun, Modulational instability and generation of envelope solitons in four-component space plasmas, *Contrib. Plasma Phys.* **58**, 870–877 (2018); doi: [10.1002/ctpp.201700069](https://doi.org/10.1002/ctpp.201700069).
 - [5] K. Singh and N. S. Saini, Breather structures and Peregrine solitons in a polarized space dusty plasma, *Front. Phys.* **8**, 602229 (2020); doi: [10.3389/fphy.2020.602229](https://doi.org/10.3389/fphy.2020.602229).
 - [6] J. Sarkar, S. Chandra, J. Goswami, and B. Ghosh, Formation of solitary structures and envelope solitons in electron acoustic wave in inner magnetosphere plasma with suprathermal ions, *Contrib. Plasma Phys.* **60**, e201900202 (2020); doi: <https://doi.org/10.1002/ctpp.201900202>.
 - [7] J. Borhanian, I. Kourakis, and S. Sobhanian, Electromagnetic envelope solitons in magnetized plasma, *Phys. Lett. A* **373**, 3667–3677 (2009); doi: <https://doi.org/10.1016/j.physleta.2009.08.010>.
 - [8] J. Borhanian, Extraordinary electromagnetic localized structures in plasmas: Modulational instability, envelope solitons, and rogue waves, *Phys. Lett. A* **379**, 595–602 (2015); doi: [http://dx.doi.org/10.1016/j.physleta.2014.12.018](https://doi.org/10.1016/j.physleta.2014.12.018).
 - [9] G. P. Veldes, J. Borhanian, M. McKerr, V. Saxena, D. J. Frantzeskakis, and I. Kourakis Electromagnetic rogue waves in beam-plasma interactions, *J. Opt.* **15** (6), 064003 (2013); doi: [10.1088/2040-8978/15/6/064003](https://doi.org/10.1088/2040-8978/15/6/064003).
 - [10] K. H. Spatschek, Coupled localized electron-plasma waves and oscillatory ion-acoustic perturbations, *The Physics of Fluids* **21**, 1032–1035 (1978); doi: <https://doi.org/10.1063/1.862323>.
 - [11] B. K. Som, M. R. Gupta, and B. Dasgupta, Coupled nonlinear Schrödinger equation for Langmuir and dispersive ion-acoustic waves, *Phys. Lett. A* **72** (2), 111–114 (1979); doi: [https://doi.org/10.1016/0375-9601\(79\)90663-7](https://doi.org/10.1016/0375-9601(79)90663-7).
 - [12] C. B. Tabi, C. S. Panguetna, T. G. Motsumi, and T. C. Kofané, Modulational instability of coupled waves in electronegative plasmas, *Phys. Scripta* **95**, 075211 (2020); doi: <https://doi.org/10.1088/1402-4896/ab8f40>.
 - [13] C. J. McKinstrie and R. Bingham, The modulational instability of coupled waves, *Phys. Fluids B: Plasma Phys.* **1**, 230–237 (1989); doi: <https://doi.org/10.1063/1.859095>.
 - [14] C. J. McKinstrie and G. G. Luther, The modulational instability of collinear waves, *Phys. Scripta* **30**, 31–40 (1990); doi: [10.1088/0031-8949/1990/T30/005](https://doi.org/10.1088/0031-8949/1990/T30/005)
 - [15] G. G. Luther and C. J. McKinstrie, Transverse modulational instability of collinear waves, *J. Opt. Soc. Am. B* **7** (6), 1125–1141 (1990); doi: <https://doi.org/10.1364/JOSAB.7.001125>
 - [16] G. G. Luther and C. J. McKinstrie, Transverse modulational instability of counterpropagating light waves, *J. Opt. Soc. Am. B* **9** (7), 1047–1060 (1992); doi: <https://doi.org/10.1364/JOSAB.9.001047>
 - [17] I. Kourakis, P. K. Shukla, and G. Morfill, Modulational instability and localized excitations involving two nonlinearly coupled upper-hybrid waves in plasmas, *New J. Phys.* **7**, 153 (2005); doi: <https://doi.org/10.1088/1367-2630/7/1/153>.
 - [18] V. Singh, Modulation instability of two laser beams in plasma, *Laser Part. Beams* **31** (4), 753–758 (2013); doi: <https://doi.org/10.1017/S0263034613000748>.
 - [19] J. Borhanian and H. A. Golijan, Copropagation of coupled laser pulses in magnetized plasmas: Modulational instability and coupled solitons, *Phys. Plasmas* **24**, 033116 (2017); doi: <https://doi.org/10.1063/1.4978576>.
 - [20] S. V. Manakov, On the theory of two-dimensional stationary self-focusing of electromagnetic waves, *Sov. Phys.-JETP* **38** (2), 248–253 (1974);
 - [21] R. Radhakrishnan and M. Lakshmanan, Bright and dark soliton solutions to coupled nonlinear Schrödinger equations, *J. Phys. A: Math. Gen.* **28**, 2683 (1995); doi: [10.1088/0305-4470/28/9/025](https://doi.org/10.1088/0305-4470/28/9/025).
 - [22] H. Bailung, S. K. Sharma, and Y. Nakamura, Observation of Peregrine solitons in a multicomponent plasma with negative ions, *Phys. Rev. Lett.* **107**, 255005 (2011); doi: <https://doi.org/10.1103/PhysRevLett.107.255005>.
 - [23] P. Pathak, S. K. Sharma, Y. Nakamura, and H. Bailung, Observation of second order ion acoustic Peregrine breather in multicomponent plasma with negative ions, *Phys. Plasmas* **23**, 022107 (2016); doi: <https://doi.org/10.1063/1.4978576>.

<http://dx.doi.org/10.1063/1.4941968>.

- [24] Yuchen He, A. Slunyaev, N. Mori, and A. Chabchoub Experimental evidence of nonlinear focusing in standing water waves, *Phys. Rev. Lett.* **129**, 144502 (2022); doi: <https://doi.org/10.1103/PhysRevLett.129.144502>
- [25] E. Infeld and G. Rowlands, *Nonlinear Waves, Solitons and Chaos*. Cambridge University Press, 1990. isbn: 0521379377.
- [26] A. V. Mikhailov, The reduction problem and the inverse scattering method, *Physica D* **3 (1-2)**, 73–117 (1981); doi: [https://doi.org/10.1016/0167-2789\(81\)90120-2](https://doi.org/10.1016/0167-2789(81)90120-2).
- [27] Freddy P. Zen and Hendry I. Elim, Soliton solution of the integrable coupled nonlinear Schrödinger equation of Manakov type, arXiv: hep-th.9812215v2 (1998); doi: <https://doi.org/10.48550/arXiv.hep-th/9812215>.
- [28] V. S. Gerdjikov, *Basic Aspects of Soliton Theory*, Proceedings of the Sixth International Conference on Geometry, Integrability and Quantization, Varna, Bulgaria, 3-10 June 2004, edited by I. M. Mladenov and A. C. Hirshfeld (Softex, Sofia, 2005), pp. 78-125; doi: <https://doi.org/10.7546/giq-6-2005-78-125>.
- [29] Deng-Shan Wang, Da-Jun Zhang, and Jianke Yang, Integrable properties of the general coupled nonlinear Schrödinger equations, *J. Math. Phys.* **51**, 023510 (2010); doi: <https://doi.org/10.1063/1.3290736>.
- [30] M. J. Ablowitz and T. P. Horikis, Interacting nonlinear wave envelopes and rogue wave formation in deep water, *Phys. Fluids* **27**, 012107 (2015); doi: <https://doi.org/10.1063/1.4906770>.
- [31] I. Kourakis and P. K. Shukla, Modulational instability in asymmetric coupled wave functions, *Eur. Phys. J. B* **50**, 321–325 (2006); doi: <https://doi.org/10.1140/epjb/e2006-00106-1>.
- [32] G. P. Veldes, J. Cuevas, P. G. Kevrekidis, and D. J. Frantzeskakis, Coupled backward- and forward-propagating solitons in a composite right- and left-handed transmission line, *Phys. Rev. E* **88**, 013203 (2013), doi: <https://doi.org/10.1103/PhysRevE.88.013203>.
- [33] N. Lazarides and G. P. Tsironis, Coupled nonlinear Schrödinger field equations for electromagnetic wave propagation in nonlinear left-handed materials, *Phys. Rev. E* **71**, 036614 (2005); doi: <https://doi.org/10.1103/PhysRevE.71.036614>.
- [34] V. V. Tyutin, Extended vector solitons with significantly different frequencies of the polarization components, *JETP Letters* **115 (10)**, 634–637 (2022); doi: <https://doi.org/10.1134/S0021364022600690>.
- [35] Y. S. Kivshar and S. K. Turitsyn, Vector dark solitons, *Opt. Lett.* **18 (5)**, 337–339 (1993); doi: <https://doi.org/10.1038/srep20785>.
- [36] B. Frisquet, B. Kibler, P. Morin, and F. Baronio, Optical dark rogue wave, *Sci. Rep.* **6**, 20785 (2016); doi: <https://doi.org/10.1038/srep20785>.
- [37] P. G. Kevrekidis and D. J. Frantzeskakis, Solitons in coupled nonlinear Schrödinger models: A survey of recent developments, *Rev. Phys.* **1**, 140–153 (2016); doi: <http://dx.doi.org/10.1016/j.revip.2016.07.002>.
- [38] N. Vishnu Priya, M. Senthilvelan, and M. Lakshmanan, Akhmediev breathers, Ma solitons, and general breathers from rogue waves: A case study in the Manakov system, *Phys. Rev. E* **88**, 022918 (2013); doi: <https://doi.org/10.1103/PhysRevE.88.022918>.
- [39] V. E. Zakharov and E. I. Schulman, To the integrability of the system of two coupled nonlinear Schrödinger equations, *Physica D* **4**, 270–274 (1982); doi: [https://doi.org/10.1016/0167-2789\(82\)90068-9](https://doi.org/10.1016/0167-2789(82)90068-9).
- [40] T. Kanna, M. Lakshmanan, P. Tchofo Dinda, and N. Akhmediev, Soliton collisions with shape change by intensity redistribution in mixed coupled nonlinear Schrödinger equations, *Phys. Rev. E* **73**, 026604 (2006); doi: <https://doi.org/10.1103/PhysRevE.73.026604>.
- [41] B. Tan and J. P. Boyd, Coupled-mode envelope solitary waves in a pair of cubic Schrödinger equations with cross modulation: Analytical solution and collisions with applications to Rossby waves, *Chaos, Solitons & Fractals* **11**, 1113–1129 (2000); doi: [https://doi.org/10.1016/S0960-0779\(99\)00016-8](https://doi.org/10.1016/S0960-0779(99)00016-8).
- [42] R. E. Ergun, C. W. Carlson, J. P. McFadden, J. H. Clemmons, and M. H. Boehm, Existence of a transverse Langmuir modulational instability in a space plasma, *Geophys. Res. Lett.* **18 (7)**, 1177–1180 (1991); doi: <https://doi.org/10.1029/91GL01563>.
- [43] J. Bonnell, P. Kintner, J.-E. Wahlund, and J. A. Holtet, Modulated Langmuir waves: Observations from Freja and SCIFER, *J. Geophys. Res.* **102 (A8)**, 17233–17240 (1997); doi: <https://doi.org/10.1029/97JA01499>.
- [44] J. C. Weatherall, Modulational instability, mode conversion, and radio emission in the magnetized pair plasma of pulsars, *Astrophys. J.* **483**, 402–413 (1997); doi: <https://dx.doi.org/10.1086/304222>.
- [45] M. S. Ruderman, Freak waves in laboratory and space plasmas, *Eur. Phys. J. Special Topics* **185**, 57–66 (2010); doi: [10.1140/epjst/e2010-01238-7](https://doi.org/10.1140/epjst/e2010-01238-7).
- [46] N. Lazarides and Ioannis Kourakis, Modulational Wave-Wave Interactions in Non-Maxwellian Plasma Fluids, Abstract No: 03-1018, presented at 20th Int. Congress on Plasma Physics (ICPP), held in Nov. 27 – Dec. 2, 2022 at Gyeongju, Korea.

Appendix A: Detailed algebraic procedure

1. Multiple scales perturbation technique

We introduce fast and slow variables, viz. $x_n = \varepsilon^n x$ and $t_n = \varepsilon^n t$ (for $n = 0, 1, 2, 3, \dots$), where $\varepsilon \ll 1$ is a small real constant, so that the partial derivatives in Eqs. (2) are approximated as

$$\frac{\partial}{\partial t} \rightarrow \frac{\partial}{\partial t_0} + \varepsilon \frac{\partial}{\partial t_1} + \varepsilon^2 \frac{\partial}{\partial t_2} + \varepsilon^3 \frac{\partial}{\partial t_3} + \dots, \quad \frac{\partial}{\partial x} \rightarrow \frac{\partial}{\partial x_0} + \varepsilon \frac{\partial}{\partial x_1} + \varepsilon^2 \frac{\partial}{\partial x_2} + \varepsilon^3 \frac{\partial}{\partial x_3} + \dots, \quad (\text{A1})$$

hence

$$\frac{\partial^2}{\partial x^2} \rightarrow \frac{\partial^2}{\partial x_0^2} + \varepsilon \left(2 \frac{\partial^2}{\partial x_0 \partial x_1} \right) + \varepsilon^2 \left(\frac{\partial^2}{\partial x_1^2} + 2 \frac{\partial^2}{\partial x_0 \partial x_2} \right) + \varepsilon^3 \left(2 \frac{\partial^2}{\partial x_0 \partial x_3} + 2 \frac{\partial^2}{\partial x_1 \partial x_2} \right) + \dots, \quad (\text{A2})$$

The dependent variables n , u , and ϕ can be expanded in powers of ε as

$$n = 1 + \varepsilon n_1 + \varepsilon^2 n_2 + \varepsilon^3 n_3 + \dots, \quad u = \varepsilon u_1 + \varepsilon^2 u_2 + \varepsilon^3 u_3 + \dots, \quad \phi = \varepsilon \phi_1 + \varepsilon^2 \phi_2 + \varepsilon^3 \phi_3 + \dots. \quad (\text{A3})$$

The expansions Eq. (A3) are substituted into Eqs. (2), and using the approximations (A1) and (A2) for the derivatives we obtain sets of equations at different orders in ε , proceeding up to order ε^3 .

Specifically, the equations in the first order ($\propto \varepsilon^1$) read

$$\frac{\partial n_1}{\partial t_0} + \frac{\partial(u_1)}{\partial x_0} = 0, \quad \frac{\partial u_1}{\partial t_0} + \frac{\partial \phi_1}{\partial x_0} = 0, \quad \frac{\partial^2 \phi_1}{\partial x_0^2} + n_1 - c_1 \phi_1 = 0, \quad (\text{A4})$$

where $x_0 = x$ and $t_0 = t$. In these equations, the following *Ansatz* is introduced

$$S_1 = S_{1,1}^{(-1)} e^{-i\theta_1} + S_{1,1}^{(1)} e^{+i\theta_1} + S_{1,2}^{(-1)} e^{-i\theta_2} + S_{1,2}^{(1)} e^{+i\theta_2}, \quad (\text{A5})$$

where $S_1 = \{n_1, u_1, \phi_1\}$ is the state vector (triplet) to 1st order, and the phases are given by $\theta_j = k_j x - \omega_j t$, with k_j and ω_j being the wavevector and the corresponding frequency of the j -th wave; note that reality of the state variables imposes $S_{1,j}^{(-1)} = (S_{1,j}^{(1)})^*$ (for $j = 1, 2$), where the star (*) denotes the complex conjugate. Note that the derivatives with respect to the fast variables $t = t_0$ and $x = x_0$ that appear in Eqs. (A4) do not act on the amplitudes $S_{1,j}^{(\pm 1)}$, since the latter does not depend on t and x . After some straightforward calculations we get the equations

$$-\omega_j n_{1,j}^{(1)} + k_j u_{1,j}^{(1)} = 0, \quad -\omega_j u_{1,j}^{(1)} + k_j \phi_{1,j}^{(1)} = 0, \quad +n_{1,j}^{(1)} - (k_j^2 + c_1) \phi_{1,j}^{(1)} = 0, \quad (\text{A6})$$

with $j = 1, 2$. Clearly, the equations for $j = 1$ are not coupled to those with $j = 2$ and thus the two waves do not interact to each other at this order of approximation. As a result, two uncoupled 3×3 systems with unknowns $(n_{1,1}^{(1)}, u_{1,1}^{(1)}, \phi_{1,1}^{(1)})$, and $(n_{1,2}^{(1)}, u_{1,2}^{(1)}, \phi_{1,2}^{(1)})$, respectively, are obtained of the form

$$\begin{bmatrix} -i\omega_j & +ik_j & 0 \\ 0 & -i\omega_j & +ik_j \\ 1 & 0 & -(k_j^2 + c_1) \end{bmatrix} \begin{bmatrix} n_{1,j}^{(1)} \\ u_{1,j}^{(1)} \\ \phi_{1,j}^{(1)} \end{bmatrix} = \begin{bmatrix} 0 \\ 0 \\ 0 \end{bmatrix}, \quad (\text{A7})$$

with $j = 1, 2$. For these systems to have a non-trivial solution, it is required that their determinants should vanish, i.e.,

$$D_j = \begin{vmatrix} -\omega_j & +k_j & 0 \\ 0 & -\omega_j & +k_j \\ 1 & 0 & -(k_j^2 + c_1) \end{vmatrix} = 0, \quad (\text{A8})$$

which provides the linear frequency dispersion relations and the corresponding group velocities as

$$\omega_j = \frac{k_j}{\sqrt{k_j^2 + c_1}}, \quad v_{g,j} = \frac{\partial \omega_j}{\partial k_j} = \frac{c_1}{(k_j^2 + c_1)^{3/2}}. \quad (\text{A9})$$

(Note that only the positive branch for both ω and k is considered.) In the following, the wavenumbers k_j and their corresponding frequency ω_j will appear in the derived mathematical expressions. This is done only for convenience and for ease in the presentation and wherever it occurs, it is implied that ω_j is provided by Eq. (12) as a function of k_j .

The systems of Eqs. (A7) can now be solved in terms of the variables $\phi_{1,j}^{(1)} = \Psi_j$ ($j = 1, 2$) to give

$$n_{1,j}^{(1)} = \left(\frac{k_j}{\omega_j}\right)^2 \Psi_j, \quad u_{1,j}^{(1)} = \frac{k_j}{\omega_j} \Psi_j, \quad \phi_{1,j}^{(1)} = \Psi_j. \quad (\text{A10})$$

The equations in the second order in ε read

$$\frac{\partial n_2}{\partial t_0} + \frac{\partial(u_2)}{\partial x_0} = \mathcal{F}_1, \quad \frac{\partial u_2}{\partial t_0} + \frac{\partial \phi_2}{\partial x_0} = \mathcal{F}_2, \quad \frac{\partial^2 \phi_2}{\partial x_0^2} - c_1 \phi_2 + n_2 = \mathcal{F}_3, \quad (\text{A11})$$

where

$$\mathcal{F}_1 = -\frac{\partial(n_1)}{\partial t_1} - \frac{\partial(u_1)}{\partial x_1} - \frac{\partial(n_1 u_1)}{\partial x_0}, \quad \mathcal{F}_2 = -\frac{\partial u_1}{\partial t_1} - \frac{\partial \phi_1}{\partial x_1} - u_1 \frac{\partial u_1}{\partial x_0}, \quad \mathcal{F}_3 = +c_2 \phi_1^2 - 2 \frac{\partial^2 \phi_1}{\partial x_0 \partial x_1} \quad (\text{A12})$$

The right-hand sides of Eqs. (A11), i.e., the function \mathcal{F}_1 , \mathcal{F}_2 , and \mathcal{F}_3 , are known functions of the leading order potential amplitudes Ψ_j that result from substitution of Eqs. (A10) into Eqs. (A12). Then, in order to solve Eqs. (A11), we use the following *Ansatz*

$$S_2 = S_2^{(0)} + \left\{ S_{2,1}^{(1)} e^{i\theta_1} + S_{2,1}^{(2)} e^{2i\theta_1} + S_{2,2}^{(1)} e^{i\theta_2} + S_{2,2}^{(2)} e^{2i\theta_2} + S_{2,+}^{(1)} e^{i(\theta_1+\theta_2)} + S_{2,-}^{(1)} e^{2i(\theta_1-\theta_2)} + C.C. \right\}, \quad (\text{A13})$$

where S = any of n , u or ϕ , and $C.C.$ denotes the complex conjugate of the expression within the curly brackets. By substitution of Eqs. (A13) into Eqs. (A11), we obtain the system of equations

$$\begin{aligned} -\omega_j n_{2,j}^{(1)} + k_j u_{2,j}^{(1)} &= -\left(\frac{k_j}{\omega_j}\right)^2 \frac{\partial \Psi_j}{\partial t_1} - \frac{k_j}{\omega_j} \frac{\partial \Psi_j}{\partial x_1} = \mu_{1,j}, & -\omega_j u_{2,j}^{(1)} + k_j \phi_{2,j}^{(1)} &= -\frac{k_j}{\omega_j} \frac{\partial \Psi_j}{\partial t_1} - \frac{\partial \Psi_j}{\partial x_1} = \mu_{2,j}, \\ & & -(k_j^2 + c_1) \phi_{2,j}^{(1)} + n_{2,j}^{(1)} &= -2ik_j \frac{\partial \Psi_j}{\partial x_1} = \mu_{3,j} \end{aligned} \quad (\text{A14})$$

resulting from all terms proportional to $e^{i\theta_1}$ and $e^{i\theta_2}$, respectively, which will be discussed later. Evaluating the action of the derivatives, one obtains an algebraic system in the form

$$-2\omega_j n_{2,j}^{(2)} + 2k_j u_{2,j}^{(2)} = -2k_j n_{1,j}^{(1)} u_{1,j}^{(1)}, \quad -2\omega_j u_{2,j}^{(2)} + 2k_j \phi_{2,j}^{(2)} = -k_j u_{1,j}^{(1)2}, \quad -(4k_j^2 + c_1) \phi_{2,j}^{(2)} + n_{2,j}^{(2)} = c_2 \Psi_j^2, \quad (\text{A15})$$

for $j = 1$ and 2 , resulting from all terms proportional to $e^{2i\theta_1}$ and $e^{2i\theta_2}$, respectively, with solutions

$$n_{2,j}^{(2)} = C_{n,2,j}^{(2)} \Psi_j^2, \quad u_{2,j}^{(2)} = C_{u,2,j}^{(2)} \Psi_j^2, \quad \phi_{2,j}^{(2)} = C_{\phi,2,j}^{(2)} \Psi_j^2, \quad (\text{A16})$$

where the coefficients are given in the Appendix, and

$$-(\omega_1 + \omega_2) n_{2,+}^{(1)} + (k_1 + k_2) u_{2,+}^{(1)} = -(k_1 + k_2) \frac{k_1 k_2}{\omega_1 \omega_2} \left(\frac{k_1}{\omega_1} + \frac{k_2}{\omega_2} \right) \Psi_1 \Psi_2 = f_1^{(+)} \Psi_1 \Psi_2, \quad (\text{A17})$$

$$-(\omega_1 + \omega_2) u_{2,+}^{(1)} + (k_1 + k_2) \phi_{2,+}^{(1)} = -(k_1 + k_2) \frac{k_1 k_2}{\omega_1 \omega_2} \Psi_1 \Psi_2 = f_2^{(+)} \Psi_1 \Psi_2, \quad (\text{A18})$$

$$-[(k_1 + k_2)^2 + c_1] \phi_{2,+}^{(2)} + n_{2,+}^{(1)} = +2c_2 \Psi_1 \Psi_2 = f_3^{(+)} \Psi_1 \Psi_2, \quad (\text{A19})$$

and

$$-(\omega_1 - \omega_2) n_{2,-}^{(1)} + (k_1 - k_2) u_{2,-}^{(1)} = -(k_1 - k_2) \frac{k_1 k_2}{\omega_1 \omega_2} \left(\frac{k_1}{\omega_1} + \frac{k_2}{\omega_2} \right) \Psi_1 \Psi_2^* = f_1^{(-)} \Psi_1 \Psi_2^*, \quad (\text{A20})$$

$$-(\omega_1 - \omega_2) u_{2,-}^{(1)} + (k_1 - k_2) \phi_{2,-}^{(1)} = -(k_1 - k_2) \frac{k_1 k_2}{\omega_1 \omega_2} \Psi_1 \Psi_2^* = f_2^{(-)} \Psi_1 \Psi_2^*, \quad (\text{A21})$$

$$-[(k_1 - k_2)^2 + c_1] \phi_{2,-}^{(2)} + n_{2,-}^{(1)} = +2c_2 \Psi_1 \Psi_2^* = f_3^{(-)} \Psi_1 \Psi_2^*. \quad (\text{A22})$$

The last two 3×3 systems result from the terms proportional to $e^{i(\theta_1+\theta_2)}$ and $e^{i(\theta_2-\theta_2)}$, respectively. Their solution reads

$$n_{2,+}^{(1)} = C_{n,2,+}^{(1)} \Psi_1 \Psi_2, \quad u_{2,+}^{(1)} = C_{u,2,+}^{(1)} \Psi_1 \Psi_2, \quad \phi_{2,+}^{(1)} = C_{\phi,2,+}^{(1)} \Psi_1 \Psi_2, \quad (\text{A23})$$

$$n_{2,-}^{(1)} = C_{n,2,-}^{(1)} \Psi_1 \Psi_2^*, \quad u_{2,-}^{(1)} = C_{u,2,-}^{(1)} \Psi_1 \Psi_2^*, \quad \phi_{2,-}^{(1)} = C_{\phi,2,-}^{(1)} \Psi_1 \Psi_2^*, \quad (\text{A24})$$

where again the coefficients $C_{n,2,\pm}^{(1)}$, $C_{u,2,\pm}^{(1)}$, and $C_{\phi,2,\pm}^{(1)}$ are given in the Appendix.

Note that, at order ε^2 , we also obtain an equation that contains the zeroth-order (“constant”) terms, i.e. terms which do not depend on the zeroth order independent variables $x = x_0$ and $t = t_0$, as

$$-c_1 \phi_2^{(0)} + n_2^{(0)} = +2c_2 (|\Psi_1|^2 + |\Psi_2|^2), \quad (\text{A25})$$

which will be used in the next subsection.

Before moving on to the third order equations in ε , we return to the discussion of the solution of Eqs. (A14). The latter, which actually consist of two 3×3 uncoupled systems for the variables $\{n_{2,1}^{(1)}, u_{2,1}^{(1)}, \phi_{2,1}^{(1)}\}$ and $\{n_{2,2}^{(1)}, u_{2,2}^{(1)}, \phi_{2,2}^{(1)}\}$, can be written in matrix form as

$$\begin{bmatrix} -\omega_j & +k_j & 0 \\ 0 & -\omega_j & +k_j \\ 1 & 0 & -(k_j^2 + c_1) \end{bmatrix} \begin{bmatrix} n_{2,j}^{(1)} \\ u_{2,j}^{(1)} \\ \phi_{2,j}^{(1)} \end{bmatrix} = \begin{bmatrix} \mu_{1,j} \\ \mu_{2,j} \\ \mu_{3,j} \end{bmatrix}, \quad (\text{A26})$$

where $\mu_{m,j}$ ($m = 1, 2, 3$ and $j = 1, 2$) are defined in Eq. (A14). Note that the determinants of the two inhomogeneous systems of Eqs. (A26) are zero, since this was a compatibility requirement imposed in the first order, that led to the frequency dispersion relations. Thus, in order to find nontrivial solutions for the two inhomogeneous systems of Eqs. (A26), it must be imposed that the following determinants

$$D'_j = \begin{vmatrix} \mu_{1,j} & +k_j & 0 \\ \mu_{2,j} & -\omega_1 & +k_j \\ \mu_{3,j} & 0 & -(k_j^2 + c_1) \end{vmatrix} = 0 \quad (\text{A27})$$

should also vanish. These determinants result from the replacement of the first column of the determinant D_j with the vector $\mu_j = [\mu_{1,j} \mu_{2,j} \mu_{3,j}]^T$. After some algebra, we obtain that in order for D'_j to vanish, the conditions

$$\frac{\partial \Psi_j}{\partial t_1} = -v_{g,j} \frac{\partial \Psi_j}{\partial x_1} \quad (\text{A28})$$

should hold (compatibility conditions). Recall that the group velocity, defined earlier, naturally arose through the compatibility conditions appearing in this order. Physically speaking, this means that the wavepacket amplitudes move at the group velocity, as expected. This is a well known result, related with the so called Newell technique in nonlinear optics, that has been discussed e.g. in Ref. [25].

2. Derivation of the coupled CNLS equations

The equations in order ε^3 are

$$\frac{\partial n_3}{\partial t_0} + \frac{\partial (u_3)}{\partial x_0} = \mathcal{G}_1, \quad \frac{\partial u_3}{\partial t_0} + \frac{\partial \phi_3}{\partial x_0} = \mathcal{G}_2, \quad \frac{\partial^2 \phi_3}{\partial x_0^2} - c_1 \phi_3 + n_3 = \mathcal{G}_3, \quad (\text{A29})$$

where

$$\mathcal{G}_1 = -\frac{\partial (n_2)}{\partial t_1} - \frac{\partial (u_2)}{\partial x_1} - \frac{\partial (n_1)}{\partial t_2} - \frac{\partial (u_1)}{\partial x_2} - \frac{\partial (n_1 u_2 + n_2 u_1)}{\partial x_0} - \frac{\partial (n_1 u_1)}{\partial x_1}, \quad (\text{A30})$$

$$\mathcal{G}_2 = -\frac{\partial u_2}{\partial t_1} - \frac{\partial \phi_2}{\partial x_1} - \frac{\partial u_1}{\partial t_2} - \frac{\partial \phi_1}{\partial x_2} - \frac{\partial u_1 u_2}{\partial x_0} - u_1 \frac{\partial u_1}{\partial x_1}, \quad (\text{A31})$$

$$\mathcal{G}_3 = -2 \frac{\partial^2 \phi_2}{\partial x_0 \partial x_1} - 2 \frac{\partial^2 \phi_1}{\partial x_0 \partial x_2} - \frac{\partial^2 \phi_1}{\partial x_1^2} + 2c_2 \phi_1 \phi_2 + c_3 \phi_1^3. \quad (\text{A32})$$

We may now substitute into Eqs. (A29)-(A32) the following *Ansatz*

$$S_3 = S_3^{(0)} + \left\{ S_{3,1}^{(1)} e^{i\theta_1} + S_{3,1}^{(2)} e^{2i\theta_1} + S_{3,1}^{(3)} e^{3i\theta_1} + S_{3,2}^{(1)} e^{i\theta_2} + S_{3,2}^{(2)} e^{2i\theta_2} + S_{3,2}^{(3)} e^{3i\theta_2} \right. \\ \left. + S_{3,+}^{(1)} e^{i(\theta_1+\theta_2)} + S_{3,-}^{(1)} e^{2i(\theta_1-\theta_2)} + S_{3,+12}^{(1)} e^{i(\theta_1+2\theta_2)} + S_{3,-12}^{(1)} e^{i(\theta_1-2\theta_2)} \right. \\ \left. + S_{3,+21}^{(1)} e^{i(2\theta_1+\theta_2)} + S_{3,-21}^{(1)} e^{i(2\theta_1-\theta_2)} + C.C. \right\}, \quad (\text{A33})$$

where $S = n, u$ or ϕ and $C.C.$ denotes the complex conjugate of the entire expression within the curly brackets. For the $\ell = 0$ mode, we obtain two equations for the variables $n_2^{(0)}$ and $u_2^{(0)}$, which will be combined with Eq. (A25) to provide a 3×3 system with the unknowns $n_2^{(0)}$, $u_2^{(0)}$, and $\phi_2^{(0)}$, viz.

$$\frac{\partial n_2^{(0)}}{\partial t_1} + \frac{\partial u_2^{(0)}}{\partial x_1} = -2 \frac{\partial}{\partial x_1} \left[\left(\frac{k_1}{\omega_1} \right)^3 |\Psi_1|^2 + \left(\frac{k_2}{\omega_2} \right)^3 |\Psi_2|^2 \right], \quad (\text{A34})$$

$$\frac{\partial u_2^{(0)}}{\partial t_1} + \frac{\partial \phi_2^{(0)}}{\partial x_1} = - \frac{\partial}{\partial x_1} \left[\left(\frac{k_1}{\omega_1} \right)^2 |\Psi_1|^2 + \left(\frac{k_2}{\omega_2} \right)^2 |\Psi_2|^2 \right] \quad (\text{A35})$$

$$n_2^{(0)} = c_1 \phi_2^{(0)} + 2c_2 (|\Psi_1|^2 + |\Psi_2|^2), \quad (\text{A36})$$

where the relations (A10) were also used. To solve Eqs. (A34)-(A36), we shall introduce the *Ansatz*

$$\phi_2^{(0)} = C_{\phi,2,1}^{(0)} |\Psi_1|^2 + C_{\phi,2,2}^{(0)} |\Psi_2|^2, \quad u_2^{(0)} = C_{u,2,1}^{(0)} |\Psi_1|^2 + C_{u,2,2}^{(0)} |\Psi_2|^2, \quad n_2^{(0)} = C_{n,2,1}^{(0)} |\Psi_1|^2 + C_{n,2,2}^{(0)} |\Psi_2|^2, \quad (\text{A37})$$

into Eqs. (A34)-(A36) and use Eq. (A28) to determine the coefficients $C_{\phi,2,j}$, $C_{u,2,j}$ and $C_{n,2,j}$, whose analytical expressions are given in the Appendix. Finally, the equations for the (1st harmonic) mode $\ell = 1$ (to third order in ε) read

$$-i\omega_j n_{3,j}^{(1)} + ik_j u_{3,j}^{(1)} = \mathcal{R}_{1,j}, \quad -i\omega_j u_{3,j}^{(1)} + ik_j \phi_{3,j}^{(1)} = \mathcal{R}_{2,j}, \quad -(k_j^2 + c_1) \phi_{3,j}^{(1)} + n_{3,j}^{(1)} = \mathcal{R}_{3,j}, \quad (\text{A38})$$

where

$$\mathcal{R}_{1,j} = - \left(\frac{\partial n_{2,j}^{(1)}}{\partial t_1} + \frac{\partial u_{2,j}^{(1)}}{\partial x_1} + \frac{\partial n_{1,j}^{(1)}}{\partial t_2} + \frac{\partial u_{1,j}^{(1)}}{\partial x_2} \right) - ik_j \left(n_{1,j}^{(-1)} u_{2,j}^{(2)} + n_{1,j}^{(1)} u_2^{(0)} + n_{1,k_j}^{(-1)} u_{2,p}^{(1)} + n_{1,k_j}^{(1)} u_{2,m}^{(\ell_j)} \right) \\ - ik_j \left(u_{1,j}^{(-1)} n_{2,j}^{(2)} + u_{1,j}^{(1)} n_2^{(0)} + u_{1,k_j}^{(-1)} n_{2,p}^{(1)} + u_{1,k_j}^{(1)} n_{2,m}^{(\ell_j)} \right) \quad (\text{A39})$$

$$\mathcal{R}_{2,j} = - \left(\frac{\partial u_{2,j}^{(1)}}{\partial t_1} + \frac{\partial \phi_{2,j}^{(1)}}{\partial x_1} + \frac{\partial u_{1,j}^{(1)}}{\partial t_2} + \frac{\partial \Psi_j}{\partial x_2} \right) - ik_j \left(u_{1,j}^{(-1)} u_{2,j}^{(2)} + u_{1,j}^{(1)} u_2^{(0)} + u_{1,k_j}^{(-1)} u_{2,p}^{(1)} + u_{1,k_j}^{(1)} u_{2,m}^{(\ell_j)} \right) \quad (\text{A40})$$

$$\mathcal{R}_{3,j} = -2ik_j \left(\frac{\partial \phi_{2,j}^{(1)}}{\partial x_1} + \frac{\partial \Psi_j}{\partial x_2} \right) - \frac{\partial^2 \Psi_j}{\partial x_1^2} + 2c_2 \left(\Psi_j^* \phi_{2,j}^{(2)} + \Psi_j \phi_2^{(0)} + \Psi_{k_j}^* \phi_{2,p}^{(1)} + \Psi_{k_j} \phi_{2,m}^{(\ell_j)} \right) \\ + 3c_3 \Psi_j (|\Psi_j|^2 + 2|\Psi_{k_j}|^2) \quad (\text{A41})$$

where $j = 1, 2$, and k_j, ℓ_j defined as $\ell_1 = 1, \ell_2 = -1, k_1 = 2$, and $k_2 = 1$. By combining properly Eqs. (A38), we arrive to a new equation from which the variables $n_{3,j}^{(1)}, u_{3,j}^{(1)}$ and $\phi_{3,j}^{(1)}$ have been eliminated (essentially, a condition for annihilation of secular terms) in the form

$$-i\omega_j \mathcal{R}_{1,j} - ik_j \mathcal{R}_{2,j} + \omega_j^2 \mathcal{R}_{3,j} = 0, \quad (\text{A42})$$

where the expressions for $\mathcal{R}_{m,j}$ ($m = 1, 2, 3$ and $j = 1, 2$) were given by Eqs. (A39)-(A41) above. By substituting the expressions for $\mathcal{R}_{m,j}$ into Eq. (A42) and using the obtained solutions for the perturbative harmonic amplitude corrections (for various harmonics and orders) $n_{1,j}^{(1)}, u_{1,j}^{(1)}, \phi_{1,j}^{(1)} = \Psi_j, n_{2,j}^{(2)}, u_{2,j}^{(2)}, \phi_{2,j}^{(2)}$,

$n_2^{(0)}$, $u_2^{(0)}$, and $\phi_2^{(0)}$, we end up after tedious and lengthy calculations with the equations

$$4\omega_1 k_1 \frac{\partial^2 \Psi_1}{\partial t_1 \partial x_1} - \frac{k_1^2}{\omega_1^2} \frac{\partial^2 \Psi_1}{\partial t_1^2} + (1 - \omega_1^2) \frac{\partial^2 \Psi_1}{\partial x_1^2} + 2i \frac{k_1^2}{\omega_1} \frac{\partial \Psi_1}{\partial t_2} + 2ik_1(1 - \omega_1^2) \frac{\partial \Psi_1}{\partial x_2} + \left(\tilde{Q}_{11} |\Psi_1|^2 + \tilde{Q}_{12} |\Psi_2|^2 \right) \Psi_1 = 0, \quad (\text{A43})$$

$$4\omega_2 k_2 \frac{\partial^2 \Psi_2}{\partial t_1 \partial x_1} - \frac{k_2^2}{\omega_2^2} \frac{\partial^2 \Psi_2}{\partial t_1^2} + (1 - \omega_2^2) \frac{\partial^2 \Psi_2}{\partial x_1^2} + 2i \frac{k_2^2}{\omega_2} \frac{\partial \Psi_2}{\partial t_2} + 2ik_2(1 - \omega_2^2) \frac{\partial \Psi_2}{\partial x_2} + \left(\tilde{Q}_{21} |\Psi_1|^2 + \tilde{Q}_{22} |\Psi_2|^2 \right) \Psi_2 = 0, \quad (\text{A44})$$

where

$$\tilde{Q}_{jj} = -2 \frac{k_j^3}{\omega_j} \left(C_{u,2,j}^{(2)} + C_{u,2,j}^{(0)} \right) - k_j^2 \left(C_{n,2,j}^{(2)} + C_{n,2,j}^{(0)} \right) + 2c_2 \omega_j^2 \left(C_{\phi,2,j}^{(2)} + C_{\phi,2,j}^{(0)} \right) + 3c_3 \omega_j^2, \quad (\text{A45})$$

and

$$\tilde{Q}_{12} = -2 \frac{k_1^3}{\omega_1} C_{u,2,2}^{(0)} - k_1 \frac{k_2}{\omega_2} \left(\omega_1 \frac{k_2}{\omega_2} + k_1 \right) \left(C_{u,2,p}^{(1)} + C_{u,2,m}^{(1)} \right) - k_1^2 C_{n,2,2}^{(0)} - \omega_1 k_1 \frac{k_2}{\omega_2} \left(C_{n,2,p}^{(1)} + C_{n,2,m}^{(1)} \right) + 2c_2 \omega_1^2 \left(C_{\phi,2,2}^{(0)} + C_{\phi,2,p}^{(1)} + C_{\phi,2,m}^{(1)} \right) + 6c_3 \omega_1^2, \quad (\text{A46})$$

$$\tilde{Q}_{21} = -2 \frac{k_2^3}{\omega_2} C_{u,2,1}^{(0)} - k_2 \frac{k_1}{\omega_1} \left(\omega_2 \frac{k_1}{\omega_1} + k_2 \right) \left(C_{u,2,p}^{(1)} + C_{u,2,m}^{(1)} \right) - k_2^2 C_{n,2,1}^{(0)} - \omega_2 k_2 \frac{k_1}{\omega_1} \left(C_{n,2,p}^{(1)} + C_{n,2,m}^{(1)} \right) + 2c_2 \omega_2^2 \left(C_{\phi,2,1}^{(0)} + C_{\phi,2,p}^{(1)} + C_{\phi,2,m}^{(1)} \right) + 6c_3 \omega_2^2. \quad (\text{A47})$$

Note that the terms proportional to the variables $n_{2,j}^{(1)}$, $u_{2,j}^{(1)}$, and $\phi_{2,j}^{(1)}$ were eliminated with the help of Eqs. (A14).

Applying the second-order compatibility conditions to simplify Eqs. (A43) and (A44), we obtain a pair of coupled NLS equations in the form of Eqs. (9)-(10).

Appendix B: Coefficients in the calculation – analytical expressions

$$C_{n,2,j}^{(2)} = \frac{(k_j^2 + c_1)}{6k_j^2} [3(4k_j^2 + c_1)(k_j^2 + c_1) - 2c_2], \quad (\text{B1})$$

$$C_{u,2,j}^{(2)} = \frac{\sqrt{k_j^2 + c_1}}{6k_j^2} [3(k_j^2 + c_1)(2k_j^2 + c_1) - 2c_2], \quad (\text{B2})$$

$$C_{\phi,2,j}^{(2)} = \frac{1}{6k_j^2} [3(k_j^2 + c_1)^2 - 2c_2], \quad (\text{B3})$$

$$C_{n,2,\pm}^{(1)} = \frac{1}{D_{\pm}} \left\{ [(k_1 \pm k_2)^2 + c_1] \left[(k_1 \pm k_2) f_2^{(\pm)} + (\omega_1 \pm \omega_2) f_1^{(\pm)} \right] + (k_1 \pm k_2)^2 f_3^{(\pm)} \right\},$$

$$C_{u,2,\pm}^{(1)} = \frac{1}{D_{\pm}} \left\{ (k_1 \pm k_2) \left[f_1^{(\pm)} + (\omega_1 \pm \omega_2) f_3^{(\pm)} \right] + (\omega_1 \pm \omega_2) [(k_1 \pm k_2)^2 + c_1] f_2^{(\pm)} \right\}, \quad (\text{B4})$$

$$C_{\phi,2,\pm}^{(1)} = \frac{1}{D_{\pm}} \left\{ (\omega_1 \pm \omega_2) \left[f_1^{(\pm)} + (\omega_1 \pm \omega_2) f_3^{(\pm)} \right] + (k_1 \pm k_2) f_2^{(\pm)} \right\},$$

where

$$D_{\pm} = (k_1 \pm k_2)^2 - (\omega_1 \pm \omega_2)^2 [(k_1 \pm k_2)^2 + c_1]. \quad (\text{B5})$$

The quantities $f_m^{(\pm)}$ ($m = 1, 2, 3$) are defined in Eqs. (A17)-(A22).

$$C_{n,2,j}^{(0)} = (c_1 C_{\phi,2,j}^{(0)} + 2c_2), \quad C_{u,2,j}^{(0)} = \frac{1}{v_{g,j}} \left[C_{\phi,2,j}^{(0)} + \frac{k_j^2}{\omega_j^2} \right], \quad C_{\phi,2,j}^{(0)} = \rho_j \frac{1}{1 - c_1 v_{g,j}^2}, \quad (\text{B6})$$

where

$$\rho_j = -(k_j^2 + c_1) - 2c_1 + 2c_2 v_{g,j}^2. \quad (\text{B7})$$